KBS TEKNISK RAPPORT

52

Calculations of nuclide migration in rock and porous media, penetrated by water

H Häggblom

AB Atomenergi 1977-09-14

KÄRN - BRÄNSLE - SÄKERHET

POSTADRESS: Kärnbränslesäkerhet, Fack. 102 40 Stockholm. Telefon 08-67 95 40

Calculations of nuclide migration in rock and porous media, penetrated by water.

H Häggblom

Arbetsrapport

Org enh och nr
AE – RF-77-3264

Titel och författare

Calculations of nuclide migration in rock and porous media, penetrated by water.

H Häggblom

Org enh och nr
AE – RF-77-3264

Antal ex/Antal sid

Datum
1977-09-14

Godkänd av

Utsändes till

CF	1 ex
FB	2 ex

Uppdrag för KBS P11:11

SUMMARY

Some physical and mathematical models are given for migration of nuclides in rock and porous media penetrated by water. The cases considered are thermal convection due to the decay heat from radioactive sources and transport due to the hydraulic gradient connected with the geographic structure. The model for thermal convection is highly simplified but is conservative compared to the often made adiabatic assumption which limits convection effects to a region characterized by a high ratio between buoyant and viscous forces. The piezometric head and corresponding gradients are calculated by analytic methods. It is shown that the solutions are strongly dependent upon the variation of the permeability with depth. The special features of migration in cracks are studied. A computer program, MINUTE, was developed for numerical calculations. Times for transport of some important nuclides to the ground surface were calculated using appropriate input data for representative Swedish deposition sites. Error margins are discussed.

BL 3004 b

1. INTRODUCTION

If radioactive nuclides penetrate all man-made barriers around an underground deposition, a very important barrier remains, namely the surrounding medium of rock or porous materials such as clay, sand, sandstone or limestone. The nuclides are then dissolved in water and follow the same path as the water but generally with a lower velocity. The main sources of flow are the hydraulic gradient and the thermal convection. It has been shown that diffusion is negligible as a source of transport over larger distances than a few meters [1, 2]. A comprehensive literature has been published about flow of fluids in porous materials [3, 4] and the experimental basis is also very satisfying. In Sweden, the most important ground material is, however, hard rock containing cracks of very varying dimensions. Investigations of the flow of fluid and dissolved materials in cracks have been made, for example, by Canadian and French groups [5, 6] and by C Louis in Karlsruhe in co-operation with Electricité de France [7]. In most works, mainly the effect of the hydraulic gradient were considered. Investigations of thermal convection have been made, for example by Lapwood [8] and Schimmel et al [9].

In the present work, the physical situations have been formulated so that the equations could be solved analytically. For describing the thermal convection a rather crude theoretical model has been used and the assumption was made that the temperature distribution is given by the conduction of heat through the solid medium. For the hydraulic gradient, three different sources were assumed, namely a well (3-dimensional boundaries), a number of slopes interrupted by horizontal plateaus and a fissure. The topography could then include lakes, hills, valleys and a sea. It was recognized that the penetration depth of the flow lines to a lake or the sea are strongly dependent upon the variation of permeability with depth. Therefore, a solution will be given which considers a variable permeability.

The inaccuracies in the models have been considered by using pessimistic experimental data for the calculations. The experimental data for cracks are not unequivocal because a realistic crack structure can hardly be reproduced in a laboratory and only a limited part of the structure can be investigated in field experiments. A careful consideration of the data was therefore necessary and has been fulfilled by personal contacts with experimenters.

2. NOMENCLATURE

The following notations will be used for the physical quantities. Additional notations for purely mathematical symbols will be explained in the context.

a = distance between cracks
b = crack thickness
c = thermal conductivity
g = acceleration of gravity
K = retardation factor (equilibrium constant)
K_d = distribution coefficient
K_p = permeability of a porous medium or a crack
N_i = nuclide discharge rate
p = hydrostatic pressure
t = time variable
T_L = leach time from the repository
V = mean flow rate per unit area
v_x, v_y, v_z = velocity components of liquid or nuclide
x, y, z = Cartesian space coordinates
α = coefficient of thermal expansion by volume
ϵ = porosity coefficient
κ = thermometric diffusivity of rock
λ = decay constant
μ = viscosity
ψ = piezometric head
ρ = density
θ = temperature

3. A COMPARISON BETWEEN FLOW IN A CRACK AND IN A POROUS MEDIUM

The flow of a fluid in a crack is in many respects similar to the flow in a porous medium. A very important similarity can be expressed by Darcys law [1] which can be expressed in the form

$$V = -\frac{K_p}{g} \text{ grad } \psi \qquad (3,1)$$

The permeability K_p is then expressed in m/s. If the permeability is given in darcys, the r.h.s. of Eq (3,1) should be multiplied by ρ/μ. For water at room temperature this factor is $9.68 \cdot 10^{-4}$. The piezometric head, ψ, is given by

$$\psi = gz + \int_{p_o}^{p} \frac{dp}{\rho} \qquad (3,2)$$

V is the flow rate in cubic meters per second per square meter of rock for porous materials. For an empty crack with thickness b and plane paralell sides, the expression corresponding to Eq (3,1) is given by

$$\bar{v} = -\frac{b^2}{12\,\mu} \text{ grad } \psi \qquad (3,3)$$

where $\bar{v}$ is the fluid velocity vector (see, for example, C Louis [7]).

The volumetric flow is then obtained by averaging the flows in all cracks over a large surface. If ϵ is the ratio between the crack areas and the total area, the average velocity in a single empty crack and the fluid velocity in a porous medium can both be expressed by the formula

$$\bar{v} = -\frac{K_p}{\epsilon\, g} \text{ grad } \psi \qquad (3,4)$$

It should be observed that a crack is seldom empty of solid particles and Eq (3,3) cannot be used in practical situations. If the crack is totally or partially filled with a porous medium, Eq (3,4) is of course still valid but problems arise

in connection with determining the porosity. The best way to determine the ratio K_p/ϵ seems to be measuring the fluid velocity in an individual crack with known physical characteristics. Interpolation to cracks of different characteristics may then be obtained by considering the influence of the crack width and the filling material. For an empty crack, the velocity is proportional to the square of the width. For filled cracks the velocity is a complicated function of the structure of the grains. A qualitative estimation of this dependence can be obtained by considering the permeabilities of different porous media. By theoretical investigations made mainly by Kozeny [1], the permeability for a porous medium was obtained as

$$K_p = \frac{c\,\epsilon^3}{\tau\,\Sigma^2} \tag{3,5}$$

where c is a constant depending on the geometrical shape of the cross section of the assumed capillary tubes. Σ is the specific surface of a porous material defined as the interstitial surface area of the pores per unit bulk volume of porous material. For a cubic packing of spheres with radius R, K_p is proportional to R^2. It can be expected that narrow cracks contain proportionally more small particles than broad cracks. This indicates that the velocity in an individual crack is proportional to the square of the crack width also for filled or partially filled cracks.

Without more experimental knowledge the b^2 dependence cannot be used for extrapolation of K_p/ϵ. It is customary to use K_p-values for typical rock configurations and use ϵ-values as defined from empty cracks. This method was used in the present work for narrow cracks. For broad ones the average crack distance is not connected to any measurement of the volumetric flow. But then direct velocity measurements may be used. The piezometric head, ψ, can be calculated for porous media from the expression

$$\nabla \left(\frac{K_p}{\epsilon} \nabla \psi \right) = 0 \tag{3,6}$$

This expression is valid for incompressible fluids and gives sufficient accuracy in all cases of interest for the calculation of nuclide migration. For cracks, Eq (3,6) is of course also valid if the constraints of the crack walls are considered in the solution. Assume that the crack is in a vertical plane which contains the flow lines for a porous medium. This is the case if the crack plane is perpendicular to the lake shore and this is paralell to the sea. Then, ψ is the same function for the crack as for a porous medium in the same plane. On the other hand, if the crack plane has a different direction the boundary conditions of the rock must be considered. Such calculations are meaningful only if the case considered involves cracks with well known geometric and geologic qualities. No such attempt has been made in this work. Assuming that all cracks are vertical and perpendicular to the lake and the sea gives an upper limit for the velocity of flow.

The boundary between media of different porosity requires special attention. Consider firstly a 2-dimensional case with two homogenous media, M1 and M2, where the ground surface of M1 is horizontal but the surface of M2 contains the sea and a slope. If M2 has higher porosity than M1, the water flow in M1 is enhanced and the flow in M2 is restricted by the boundary. The same situation appears for a crack which suddenly changes its dimensions. This is seldom the case. Usually, a smaller crack ends up into a larger one which goes in another direction. The difference is then that the flow in the larger crack will not be significantly affected by the smaller one. But the flow in the smaller one will still be increased by this discontinuity. If more than two such discontinuities occur, an increase in flow will occur in each crack which has its outlet before a boundary. Results for homogenous media can then be used for obtaining upper limits for the flow velocities.

The problem of thermal convection is very difficult already

for homogenous media. In this work, no attempt has been made to investigate the specific effects appearing in cracks. But it should be pointed out that a crack restricts the geometry to two dimensions and this will decrease the convection flow.

The dissolved nuclides have generally a lower velocity than the water because of the sorbtion effect. The retardation factor K is defined as the ratio of the groundwater velocity to the nuclide migration velocity. For granular media the K factor is related to a distribution coefficient K_d by the expression

$$K = 1 + \frac{K_d \rho_b}{\epsilon} \tag{3,7}$$

where ρ_b is the bulk dry density of the porous medium and ϵ is the void ratio.

For faulted media like cracks it is sometimes preferred using a surface distribution coefficient K_a in place of K_d. Then,

$$K = 1 + K_a R_f \tag{3,8}$$

where R_f is the surface to volume ratio for the fault.

Strictly, the sorbtion is always connected to a surface. For granular media the active surface is Σ, defined in connection with Eq (3,5). Thus, there is no marked difference between the sorbtion in cracks and in porous media and Eq (3,7) can be used as an alternative to Eq (3,8).

If the retardation factor K is written as

$$K = \frac{v}{v_a} \tag{3,9}$$

where v_a is the nuclide velocity, the water velocity v can

be eliminated by using Eq (3,4). From Eq (3,7) we then obtain

$$v_a = - \frac{K_p \text{ grad } \psi}{g(\epsilon + K_d \rho_b)} \qquad (3,10)$$

If $K_d \rho_b$ is large compared to ϵ, the latter quantity is negligible in calculating v_a. It is, however, difficult to obtain experimental values for $K_d \rho_b$ in cracks. If Eq (3,8) is used in place of Eq (3,7) and the surface to volume ratio in the crack is $2\Gamma/b$, where Γ is an experimental factor, the nuclide velocity is

$$v_a = - \frac{a K_p \text{ grad } \psi}{g(b + 2 \Gamma K_a)} \qquad (3,11)$$

According to Canadian estimations K_a is of the order 0.5×10^{-5} to 0.5×10^{-2} meters [5]. For an empty crack, Γ equals one. Then, b and $2 \Gamma K_a$ are sometimes of the same order. But if the crack is partially filled, Γ may be several orders of magnitude larger. If $\Gamma = 100$, the highest nuclide velocity is only 10^2 to 10^3 times the volumetric velocity, and is indepentent of the crack width.

4. ESTIMATION OF THE THERMAL CONVECTION

Thermal convection caused by a constant heat gradient has been considered by Lapwood [8]. He concluded that a steady-state convection can occur only under certain conditions, but this was for the adiabatic case with no cooling of the vertical boundaries. When heat is produced at the repository, convection must always occur. Close to the heat source, the heated fluid will expand and move upward because of its lower density compared to adjacent parts of the fluid. The vertical velocity will decrease as the temperature decreases in upward direction and because of the incompressibility of the fluid a pattern of circulation loops will arise. The fluid will of course also carry heat away from the source. The temperature at the source surface will then decrease, causing a lower initial fluid velocity,

but because the temperature is spread out the time of streaming in vertical direction will increase. This heat transport is not considered in the present work because the volumetric water flow is low and the convection model used can in any case give only an estimation of the convection effect. Further, all effects due to acceleration or retardation of the flow are neglected.

The forces acting upon a volume element of fluid are then the pressure, the resistance according to Darcys law and the gravitational force. The equation of equilibrium is given as

$$\text{grad } p + \frac{\rho \epsilon g}{K_p} \bar{v} + \rho\, g\, \bar{e}_z = 0 \qquad (4,1)$$

where $\bar{e}_z$ is the unit vector in z-direction.

For thermal changes by conduction only, the heat equation is

$$\frac{\partial \theta}{\partial t} = \kappa \nabla^2 \theta \qquad (4,2)$$

In the static case where no thermal convection occurs the state variables are given by

$$p_o = - g\, \rho_o z \qquad (4,3)$$
$$\theta_o = - \beta\, z \qquad (4,4)$$
$$\rho_o = \rho_c (1 - \alpha\, \theta_o) \qquad (4,5)$$

The heat source causes a disturbance such that

$$p = - g\, \rho_o\, z + p_1 \qquad (4,6)$$
$$\theta = - \beta\, z + \theta_1 \qquad (4,7)$$
$$\rho = \rho_c [1 - \alpha(\theta_o + \theta_1)] \qquad (4,8)$$

Inserting Eqs (4,6) and (4,8) into Eq (4,1) gives for a two-dimensional convection current

$$\frac{\partial p_1}{\partial x} + \frac{g\epsilon\rho_c}{K_p}\left[1 - \alpha(\theta_o + \theta_1)\right] v_x = 0 \qquad (4,9)$$

$$\frac{\partial p_1}{\partial z} + \frac{g\epsilon\rho_c}{K_p}\left[1 - \alpha(\theta_o + \theta_1)\right] v_z - g\,\rho_c\,\alpha\,\theta_1 = 0 \qquad (4,10)$$

where v_x and v_z are the x- and z-components of $\bar{v}$.

Consider firstly a rectangular loop of flow with constant velocity, v_c. The loop is assumed to have two vertical parts, with length 1. One of them has a temperature close to θ_o while the temperature in the other part is risen by the value θ_1. There are also two horizontal parts with length kl and average temperatures between θ_o and $\theta_o + \theta_1$. Assume further that p_1 is a linear function of x and z. Then, using Eqs (4,9) and (4,10) and neglecting terms of higher order, the velocity in the loops is obtained as

$$v_c = \frac{K_p\,\alpha\,\theta_1}{2(k+1)\epsilon} \qquad (4,11)$$

In reality, there is a continuum of loops with different velocities and different shapes. They may even be 3-dimensional. As the heat source has a non-zero extension in the horizontal plane, the loops will probably be extended in that plane, that is, the constant k in the denominator will be larger than 1. Furthermore, the temperature in the downward flow is higher than θ_o. This will counteract the convection and still increase the denominator of Eq (4,11). On the other hand, an extension to 3-dimensions will cause the flow in horizontal direction and the downward directed flow to have a lower velocity than the upward flow. This effect decreases the denominator. The net result will be dependent upon whether the flow goes in one or a few cracks or in a homogenous material. It was assumed in this work, that the flow is 2-dimensional and that the effect of the extension in horizontal direction and of the elevated temperature in the return path is such that k is equal to 3.

The error connected with uncertainties in k will be discussed in paragraph 6.5. Then

$$v_c = \frac{K_p \alpha \theta_1}{8 \epsilon} \tag{4,12}$$

The time- and space-dependent temperature θ_1 was calculated by solving Eq (4,2) for a point source. The assumption was made that the temperature at the surface of the source can be given as

$$\theta_s(r = r_o) = \sum_{i=1}^{n} \theta_{s,i}(t_i)\, e^{-\lambda_i t} \tag{4,13}$$

where $\theta_{s,i}$ is a step function starting at the time t_i and r_o is such a small radius that the heat capacity of the source can be neglected. This is of course not the true case and the λ_is were adjusted accordingly. Thus, they are not the true decay constants of the heat sources. For obtaining a more realistic description of the situation, the λ_is were chosen so that the true heat decay at the surface of the depository was simulated. This heat decay was obtained from 3-dimensional calculations made by Blomquist [14, 15].

The solution of Eq (4,2) for a spherical source with the surface temperature θ_s is

$$\theta_1 = \frac{2 r_o}{r\sqrt{\pi}} \int_0^{\infty} e^{-(u + u_o)^2} du \sum_i \theta_{s,i}\, e^{-\lambda_i t_{i,s}} \tag{4,14}$$

where

$$u_o = \frac{r - r_o}{2\sqrt{\kappa\, t}} \tag{4,15}$$

and

$$t_{i,s} = t\left[1 - \frac{u_o^2}{(u - u_o)^2}\right] - t_i \tag{4,16}$$

The integration of Eq (4,14) was made numerically. The temperature obtained for a given point in time and space was then used for calculating the vertical velocity by Eq (4,12). The meshes were chosen so small that the velocity could be assumed constant for obtaining the next point in the nuclide migration. The total velocity was of course given by superposition of the contributions from the convection and the gradient effects.

5. CALCULATION OF GRADIENT EFFECTS

5.1 Geometries and boundary conditions

The gradient effects were calculated by solving the differential equation for the piezometric head. For an incompressible fluid this is given by Eq (3,6). Purely analytical solutions were obtained by assuming appropriate boundary conditions and convenient assumptions about the space dependence of the permeability K_p. Thus, the part of ψ (x, y, z) defining the surface boundary condition was given for

$$-\infty \leqq x \leqq \infty$$
$$-\infty \leqq y \leqq \infty$$
$$z = 0$$

This means that the height variations of the ground surface were simulated by variations in ψ in the plane z = 0. This is a small restriction only, because the height variations around appropriate burial places are small compared to the average depth of the nuclide path.

At large depths, two alternative boundary conditions were used, namely,

$$\psi(x, y, -\infty) = 0 \qquad (5,1)$$

or

$$\left(\frac{\partial \psi}{\partial z}\right)_{z = -z_{max}} = 0 \qquad (5,2)$$

The restrictions in geometry and in the space dependence of the permeability were determined by the following four cases.

a) 3-dimensional calculations with the surface boundary conditions determined by a drained well with constant rectangular cross section in the horizontal plane. The ψ-function was zero at $z = -\infty$. The permeability was assumed constant. See Fig 1.

b) 2-dimensional calculations for a simplified lake or valley. Lower boundary conditions according to Eq (5,1). See Fig 2.

c) 2-dimensional calculations with surface boundary conditions appropriate to a sea with a shore slope, see Fig 3. The lower boundary condition was according to Eq (5,1) and the permeability was assumed constant.

d) 2-dimensional calculations with surface boundary conditions according to Fig 4. The topography is described by a number of slopes interrupted by horizontal surfaces. The lower boundary condition was according to Eq (5,2). The permeability was a function of depth.

5.2 A 3-dimensional solution

For constant permeability, the piezometric head obeys the Laplace equation which in 3-dimensional Cartesian coordinates can be expressed as

$$\frac{\partial^2\psi}{\partial x^2} + \frac{\partial^2\psi}{\partial y^2} + \frac{\partial^2\psi}{\partial z^2} = 0 \qquad (5,3)$$

The method of solving this equation with the boundary conditions given in paragraph 5.1 a) is explained in Appendix 1. The result is

$$\psi = \psi_1\left(\frac{x_s}{2} - x, \frac{y_s}{2} - y\right) + \psi_1\left(\frac{x_s}{2} - x, \frac{y_s}{2} + y\right) \pm$$
$$\pm \psi_1\left(\frac{x_s}{2} + x, \frac{y_s}{2} - y\right) \pm \psi_1\left(\frac{x_s}{2} + x, \frac{y_s}{2} + y\right) \qquad (5,4)$$

where

$$\psi_1(\xi, \eta) = \frac{gz_s}{4\pi^2}\left[\arcsin\left(\frac{\frac{\xi^2}{z^2} + \frac{\xi^2 - \eta^2}{\xi^2 + \eta^2}}{1 + \frac{\xi^2}{z^2}}\right) + \right.$$

$$\left. + \arcsin\left(\frac{\frac{\eta^2}{z^2} + \frac{\eta^2 - \xi^2}{\eta^2 + \xi^2}}{1 + \frac{\eta^2}{z^2}}\right)\right] \qquad (5,5)$$

x_s, y_s and z_s are the dimensions given in Fig 1. It is assumed that

$$y < \frac{y_s}{2}$$

For the two last terms of Eq (5,4), the plus-signs are valid when $|x| < x_s/2$. If $|x| > x_s/2$ the minus-signs are valid.

An idea about the behaviour of ψ is obtained by taking the partial derivative with respect to z and letting x be much larger than $y + y_s$. Then

$$\frac{\partial \psi}{\partial z} \to \frac{g\, x_s\, y_s\, z_s (x^2 - z^2)}{\pi^2 (x^2 + z^2)^{5/2}} \text{ for } x >> y + y_s \qquad (5,6)$$

Thus, the vertical flow is zero along the lines $|x| = |z|$. For smaller values of $|x|$, the flow is upward and vice versa.

This model is appropriate for a well with horizontal dimensions not too small compared to the vertical dimension. For a drilled well, the flow lines go mainly to the vertical surface and a solution of ψ in polar coordinates is more appropriate. Of course, the model can also be used for calculating the flow to a lake. But then, the flow on large depths is important and it is more convenient to consider a solution for z-dependent permeability. Such a solution will, however, be given only for a 2-dimensional case. Therefore, it is useful to investigate the y_s-dependence of the present solution.

Eq (5,5) can be written as the sum of two functions, ψ_1' and ψ_1''. The partial derivatives of the two parts of ψ_1 are, with $y_s = 2\ y_o$

$$\frac{\partial \psi_1'}{\partial \xi} = \frac{g\ z_s\ \xi}{\pi^2} \left(\frac{y_o^2}{\xi^2 + y_o^2}\right) \left(\frac{z^2}{\xi^2 + z^2}\right) \left(\frac{1}{\xi^2 + y_o^2} + \right.$$

$$\left. + \frac{1}{\xi^2 + z^2}\right) \frac{1}{\sqrt{1 - u_o^2}} \qquad (5,7)$$

$$\frac{\partial \psi_1'}{\partial z} = \frac{g\ z_s\ z}{\pi^2} \left(\frac{y_o^2}{\xi^2 + y_o^2}\right) \left(\frac{\xi}{\xi^2 + z^2}\right)^2 \frac{1}{\sqrt{1 - u_1^2}} \qquad (5,8)$$

where

$$u_1 = \frac{\xi^2 + \left(\frac{\xi^2 - y_o^2}{\xi^2 + y_o^2}\right) z^2}{\xi^2 + z^2} \qquad (5,9)$$

$$\frac{\partial \psi_1''}{\partial \xi} = -\frac{g\ z_s\ \xi}{\pi^2} \left(\frac{y_o}{\xi^2 + y_o^2}\right)^2 \left(\frac{z^2}{y_o^2 + z^2}\right) \frac{1}{\sqrt{1 - u_2^2}} \qquad (5,10)$$

$$\frac{\partial \psi_1''}{\partial z} = \frac{g\ z_s\ z}{\pi^2} \left(\frac{y_o}{\xi^2 + y_o^2}\right) \left(\frac{\xi}{y_o^2 + z^2}\right)^2 \frac{1}{\sqrt{1 - u_2^2}} \qquad (5,11)$$

where

$$u_2 = \frac{y_o^2 + \left(\frac{y_o^2 - \xi^2}{y_o^2 + \xi^2}\right) z^2}{y_o^2 + z^2} \qquad (5,12)$$

It is now evident that the gradient of ψ for $x >> x_o$ and $y_s >> x$ is proportional to the factor

$$p = \frac{y_o^2}{x^2 + y_o^2} \qquad (5,13)$$

For smaller x-values, this proportionality is still valid if $z >> y_s$. Therefore, the results for the 2-dimensional lake model have been multiplied by p in order to take care of the finite size in the y-direction. This is of course only a crude approximation. From Eq (5,6) it is evident that at least the z-derivative is proportional to y_s for $x >> y_s$ and $y = 0$.

5.3 Two-dimensional calculations of the piezometric head

For calculating the flow to a sea like the Baltic or larger, a 2-dimensional model is appropriate. Further, a solution corresponding to an exponential decrease of the permeability with the depth is easily obtainable in two dimensions.

Firstly, consider the Laplace equation with boundary conditions according to Fig 3. If the lower boundary approaches infinity, the solution is (see Appendix 1),

$$\psi(x,z) = \frac{g\, z_s}{\pi}\left[\frac{\pi}{2} - \frac{x}{x_s}\operatorname{arc\,tg}\left(\frac{x}{z}\right) + \left(\frac{x}{x_s} - 1\right)\operatorname{arc\,tg}\left(\frac{x - x_s}{z}\right) - \frac{z}{2\,x_s}\ln\left(1 + \frac{x_s^2 - 2\,xx_s}{x^2 + z^2}\right)\right] \tag{5,14}$$

The partial derivatives are

$$\frac{\partial\psi}{\partial x} = -\frac{g\, z_s}{\pi}\left\{\frac{xx_s\, z}{(x^2 + z^2)[(x - x_s)^2 + z^2]} + \frac{1}{x_s}\left[\operatorname{arc\,tg}\left(\frac{x}{z}\right) - \operatorname{arc\,tg}\left(\frac{x - x_s}{z}\right)\right]\right\} \tag{5,15}$$

$$\frac{\partial\psi}{\partial z} = \frac{g\, z_s}{2\pi\, x_s}\ln\left[\frac{x^2 + z^2}{(x - x_s)^2 + z^2}\right] \tag{5,16}$$

From Eq (5,16) it is evident that the flow is directed downward if $x < x_s/2$ and vice versa. The behaviour is therefore different to that for a 3-dimensional lake where the vertical direction was dependent of the depth. The flow to a 2-dimensional sea will reach great depths if there is no lower boundary.

A generalization will now be made, based upon the experimental fact that the permeability is a function of the depth. It decreases by two orders of magnitude from 0 to 100 m depth [10, 11]. This case will be handled under the assumption that a lower boundary is present at finite depth.

For a non-constant permeability, K_p, the piezometric head is not governed by the Laplace equation. If K_p is only a function of z, Eq (3,6) can be written

$$K_v \nabla^2 \psi + \frac{dK_v}{dz} \frac{\partial \psi}{\partial z} = 0 \qquad (5,17)$$

where

$$K_v = \frac{K_p}{\epsilon} \qquad (5,18)$$

The proper boundary conditions are different from those valid for an infinite lower space. It is not the ψ-function which is zero at some depth $-z_{max}$ because this may give rise to a non-existent vertical flow. Instead, the vertical flow is zero at the lower boundary. This corresponds to Eq (5,2).

Fig 4 shows a topography of horixontal surfaces at different heights interconnected by plane slopes. Corresponding boundary conditions are also given. Eq (5,17) is now solved for upper boundary conditions according to Fig 4, for a lower boundary condition according to Eq (5,2) and with a z-dependence of K_v given as

$$K_v = K_o \, e^{az} \tag{5,19}$$

For brevity, the quantity μ_n and the functions F (z) and G (x, z) are introduced by the expressions

$$\mu_n = \sqrt{1 + \left[\frac{a \, z_{max}}{(n - \frac{1}{2}) \, \pi}\right]^2} \, , \quad n = 1, \, 2 \ldots \tag{5,20}$$

$$F(z) = \frac{2}{\pi} \sum_{n=1}^{\infty} \frac{\sin\left[\frac{\pi(n - \frac{1}{2}) \, z}{z_{max}}\right]}{(n - \frac{1}{2}) \, \mu_n} \, e^{-\frac{az}{2}} \tag{5,21}$$

and

$$G(x, z) = \frac{z_{max} \, e^{-\frac{az}{2}}}{\pi^2} \sum_{n=1}^{\infty} \frac{\sin\left[\frac{\pi(n - \frac{1}{2}) \, z}{z_{max}}\right]}{(n - \frac{1}{2})^2 \, \mu_n^2}$$

$$\sum_{i=1}^{N} \left(\frac{z_i - z_{i+1}}{x_{2i} - x_{2i-1}}\right) \left[e^{-\frac{\pi(n - \frac{1}{2}) \, \mu_n |x_{2i-1} - x|}{z_{max}}} - \right.$$

$$\left. - e^{-\frac{\pi(n - \frac{1}{2}) \, \mu_n |x_{2i} - x|}{z_{max}}} \right] \tag{5,22}$$

where N is the number of slopes. The meaning of the quantities x_k and z_k can be found from Fig 4.

The piezometric head is then

$$\psi \, (x, \, z) = g\left[z_k \, F \, (x) + G \, (x, \, z)\right] \tag{5,23}$$

if x is inside the horizontal plane preceding slope k and

$$\psi \, (x, \, z) = g\left[z_k \left(1 - \frac{x - x_{2k-1}}{x_{2k} - x_{2k-1}}\right) F(z) + G(x, \, z)\right] \tag{5,24}$$

if x is within the boundaries given by slope k. For the last horizontal plane, z_k is zero.

If the permeability is constant, μ_n and F(z) are both equal to 1. For physical reasons, F(z) should always be constant. Otherwise there is a vertical flow even in the absence of any slopes. This vertical flow can only be present if there is a vertical boundary with non-zero crossing flow. Because no such boundary is assumed, the vertical gradient corresponding to F(z) is always set to zero. Numerical computations show that F(z) is always nearly constant. Its dependence of the permeability parameter 'a' is, however, important for calculating the horizontal flow below a slope. It is shown in Appendix 2 how the slow convergence of the sum in Eq (5,21) can be circumvented.

The variation of the permeability with depth corresponds to values of the parameter 'a' between 2 and 5. Such high values will decrease the ψ-function considerably compared to that for a constant permeability. Then, the flow velocity will decrease correspondingly for a given value of K_v. But, because the depth penetration of the flow will be smaller, the resulting change in the transport time will be dependent upon the topography. If there are no large changes in the surface gradient, the transport time will be much longer for a case with varying permeability. But in some cases the transport time is shorter for varying permeability.

The derivatives of the ψ-function contain sums which sometimes converge very slowly and they diverge for $x = x_{2i-1}$ or $x = x_{2i}$. Therefore, they were computed from finite differences of the ψ-function.

A two-dimensional lake or valley is formed if the angles of inclination of two subsequent slopes change from a negative to a positive value. A hill is obtained with the opposite change of sign. An approximate consideration of the third dimension was obtained by multiplying the gradients with the factor p given by Eq (5,13). It should,however, be kept

in mind that the flow will probably turn into the perpendicular direction when arrived at a valley. A proper consideration of this situation can only be made by 3-dimensional calculations but an approximate solution may be obtained by two subsequent 2-dimensional calculations in different directions.

The experiments referred to earlier in this paragraph show that the permeability will approach a constant value for large depths. Therefore, the solutions for an exponentially decaying permeability are not very good even if the decay constant 'a' is fitted to some K-value at an average depth of flow. It can, however, be easily shown that a combination of the solutions for constant permeability and for an exponentially decaying permeability will be good improvement. Consider a K_v-function of the type

$$K_v = K_o + K_1 e^{az} \tag{5,25}$$

The corresponding transport equation is

$$(K_o + K_1 e^{az}) \nabla^2 \psi + a K_1 e^{az} \frac{\partial \psi}{\partial z} = 0 \tag{5,26}$$

For $z \to 0$, Eq (5,26) approaches the equation

$$(K_o + K_1) \nabla^2 \psi + a K_1 \frac{\partial \psi}{\partial z} = 0 \tag{5,27}$$

This has the same form as the equation for experimentally decaying permeability. Call the solution ψ_1. For $z \to -\infty$, Eq (5,26) approaches the equation for constant permeability. Call the corresponding solution ψ_2. A convenient approximation to the solution of Eq (5,26) is then a linear combination of the solution of Eq (5,27) and that for constant permeability, that is,

$$\psi = A \psi_1 + B \psi_2 \tag{5,28}$$

The constants a, A and B are obtained from the K-value at $z = 0$, K_{zo}, at $z = -1$, K_{z1}, and at $z = -\infty$, K_∞. It is easily seen that

$$a = \frac{\gamma(K_{zo} - K_\infty)}{K_{zo}} \tag{5,29}$$

where

$$\gamma = \ln\left(\frac{K_{zo} - K_\infty}{K_{z1} - K_\infty}\right) \tag{5,30}$$

A and B were calculated so that $\psi = \psi_2$ for a constant permeability and $\psi = \psi_1$ for a pure exponential decay. Then,

$$A = \frac{K_{zo} - K_\infty}{K_{zo}} \tag{5,31}$$

$$B = \frac{K_\infty}{K_{zo}} \tag{5,32}$$

In practical situations, the constant B is small compared to A.

5.4 Consideration of boundaries between media with different permeabilities

Consider firstly a 2-dimensional medium consisting of N homogenous parts. They are numbered from left to right. Assume that a solution of the ψ-function, ψ_1, is obtained for medium 1 with boundary conditions as those for an infinite medium. The geometric assumptions are such that $\psi = 0$ for $x = -\infty$ but is not necessarily zero for $x = +\infty$. Denote the x-value for the right boundary of medium 1 with x_1, that for the next boundary with x_2 and so on. For medium 2 the solution ψ_2 of the transport equation is divided into symmetric and antisymmetric components with respect to x_1. With the notion

$$x' = x - x_1 \tag{5,33}$$

ψ_2 can be written

$$\psi_2\ (x,z) = \frac{1}{2}\left[\psi_{2,s}\ (x',z) + \psi_{2,A}\ (x',z)\right] \qquad (5,34)$$

where

$$\psi_{2,s}\ (x',z) = \psi\ (x' + x_1,z) + \psi\ (-x' + x_1,z) \qquad (5,35)$$

and

$$\psi_{2,A}\ (x',z) = \psi\ (x' + x_1,z) - \psi\ (-x' + x_1,z) \qquad (5,36)$$

It is easily seen that the following conditions are valid for $x = x_1$ or $x' = 0$

$$\left(\frac{\partial\psi_{2,s}}{\partial x}\right)_{x'=0} = \left(\frac{\partial\psi_{2,A}}{\partial z}\right)_{x'=0} = 0 \qquad (5,37)$$

Now, the flow at the boundary $x' = 0$ is continous in the x- and z-directions separately. In order to fulfil this condition, the solutions are changed in the following way.

$$\psi_1\ (x,z) \rightarrow a_1\ \psi_1\ (x',z) \qquad (5,38)$$

$$\psi_2\ (x,z) \rightarrow a_{2,s}\ \psi_{2,s}\ (x',z) + a_{2,A}\ \psi_{2,A}\ (x',z) \qquad (5,39)$$

Besides the translation of the x-coordinate, the function ψ_1 is multiplied by a constant. This means that the flow lines are unchanged but the velocity of the flow is multiplied by the same constant in each point. For ψ_2, there is also a change in the flow lines which is obtained by changing the boundary conditions to the left of the line $x = x_1$. This change of boundary conditions simulates the change of permeability. It should be noted that the two solutions according to Eqs (5,35) and (5,36) are obtained from the general solution of the transport equation in the complete space with a permeability independent of x.

The flow in z-direction at the x_1 boundary is independent of the change in permeability. Therefore, using Eq (5,37)

$$a_1\left(\frac{\partial\psi_1}{\partial z}\right)_{x'=0} = a_{2,s}\left(\frac{\partial\psi_{2,s}}{\partial z}\right)_{x'=0} \tag{5,40}$$

Now, according to Eq (5,35)

$$\left(\frac{\partial\psi_{2,s}}{\partial z}\right)_{x'=0} = 2\left(\frac{\partial\psi}{\partial z}\right)_{x=x_1} = 2\left(\frac{\partial\psi_1}{\partial z}\right)_{x'=0} \tag{5,41}$$

and then

$$a_{2,s} = \frac{a_1}{2} \tag{5,42}$$

The flow in the x-direction is obtained by multiplying each x-derivative by the permeability. Thus,

$$K_{p,1}\ a_1\left(\frac{\partial\psi_1}{\partial x'}\right)_{x'=0} = K_{p,2}\ a_{2,A}\left(\frac{\partial\psi_{2,A}}{\partial x'}\right)_{x'=0} \tag{5,43}$$

where the indices on the permeabilities refer to the proper media.

Using Eqs (5,36) and (5,43), the relationship between $a_{2,A}$ and a_1 is obtained as

$$a_{2,A} = \frac{1}{2}\left(\frac{K_{p,1}}{K_{p,2}}\right) a_1 \tag{5,44}$$

The same procedure can be repeated at each new boundary in the right direction. In the Nth medium (the last to the right), a new relationship is obtained by letting x' approach infinity. Because $\psi\ (x = -\infty,\ z = 0) = 0$,

$$\psi_{N,s}\ (\infty,0) = \psi_{N,A}\ (\infty,0) = \psi\ (\infty,0) \tag{5,45}$$

Then, in order to fulfill the boundary condition at $x = \infty$, the following relationship is obtained.

$$a_{N,s} + a_{N,A} = 1 \tag{5,46}$$

The final solutions for the weighting factor can be written in a simple form by using the notion

$$\kappa = \frac{K_{p,1}}{K_{p,N}} \tag{5,47}$$

Then,

$$a_{n,s} = \frac{1}{2}\, a_1 = \frac{1}{1 + \kappa} \tag{5,48}$$

$$a_{n,A} = \frac{1}{1 + \kappa} \left(\frac{K_{p,1}}{K_{p,n}}\right) \tag{5,49}$$

If for each medium $\kappa_{n+1} >> \kappa_n$, the constant a_1 approaches 2, $a_{n,s}$ approaches 1 and $a_{n,A}$ approaches zero. The conclusion is then that the flow in each medium can never be more than 2 times the flow obtained if this medium fills the total space. The factor 2 is obtained if the permeability to the right of the medium is infinite.

If now a medium of hard rock with cracks is considered it should be noted that the flow in each crack is feeded from a number of other cracks. Then, if the first junction in the flow path followed is denoted by x_1, the flow to the right of x_1 is not determined by the x-coordinate only but also of the conditions in a direction, say y_1, corresponding to the main flow in crack No 2. But even in this case it is evident that the flow to the left of point x_1 cannot be increased by more than a factor of two due to an increase in the permeability at point x_1. A reasonable but probably pessimistic estimation is obtained by multiplying the ψ-function to the left of each junction with the factor

$$a_n = \frac{2}{1 + \frac{K_{p,n}}{K_{p,N}}} \tag{5,50}$$

6. NUMERICAL CALCULATIONS

6.1 The MINUTE Computer program

MINUTE calculates the migration of a nuclide from the point of repository to the point where it reaches the surface. The velocity components due to the temperature rise and to the hydraulic gradient are calculated at a number of discrete points along the path. The first steps in time and in vertical direction are given in the input data but later time steps are chosen by the program so that each vertical step is not greater than 3 times the first vertical step and not smaller than this step. The steps in space are then obtained as the vector sum of the product of velocity components and time step.

The thermal convection is calculated from the formulas given in section 4 and the gradient effects due to a well or a lake and to a sea are calculated according to the theory given in section 5. A constant horizontal flow can be superposed upon the results. For one lake or one valley the perpendicular dimension can be considered approximately. Otherwise lakes and valleys are treated by the 2-dimensional model. For a well, the 3-dimensional solution of the piezometric head for constant permeability is used.

The nuclide leach time from the repository, T_L, is divided into an arbitrary number of time steps with a given weight function. The migration is calculated for the beginning of each step and the weight function is used for obtaining the corresponding discharge rate.

The input data to MINUTE are

κ = thermometric diffusivity of rock, km^2/yr

α = coefficient of thermal expansion by volume

K_p = average permeability of the rock, km/yr

K = retardation factor

λ_n = nuclide decay constant, yr^{-1}

v_h = horizontal water velocity to be superposed, km/yr

N = number of zones with different permeabilities

x_n $(n=1,N)$ = right boundary of each zone, km

$K_{zo,n}$ $(n=1,N)$ = permeability at the ground surface in km/yr for each zone

$\epsilon_{zo,n}$ = porosity at the ground surface for each zone

$K_{z1,n}$ = permeability at 1 km depth in km/yr for each zone

$\epsilon_{z1,n}$ = porosity at 1 km depth for each zone

$K_{\infty,n}$ = permeability at infinite depth in km/yr for each zone

$\epsilon_{\infty,n}$ = porosity at infinite depth for each zone

N_H = number of heat sources at the repository

$\lambda_{H,n}$ $(n=1,N_H)$ = decay constants for the heat sources yr^{-1}

$t_{s,n}$ = start times for the heat sources yrs

$\theta_{s,n}$ = initial temperatures above environment temperature for the heat sources, ^oC

T_L = nuclide leach time from repository, yrs

H_o = distance from ground water level to the center of the repository, km

z_{max} = lower boundary of the piezometric head, km

ISLOPE = 0/1: Are the slopes present, no/yes

ILAKE = 0/1: Is there a lake present, no/yes

IWELL = 0/1: Is there a well present, no/yes

NSLOPE = number of slopes present

x_{2i-1}, z_i, x_{2i}, z_{i+1} = x and z values for the left and right boundaries, respectively, of each slope. x-values in km, z-values in meters. Only present if ISLOPE = 1

XL_1, ZL_1, XL_2, ZL_2 = x and z values for the left and right boundaries, respectively, of the lake. x-values in km, z-values in meters. Only present if ILAKE = 1

RS = distance from repository to the well (km)

XS, YS = horizontal well dimensions, meters

ZS = height over sea level of the well surface, meters

WDEPTH = depth of well, meters
(The well data are only present if IWELL = 1)

R_o = distance between top and centre of the repository, km

d_z = initial step in vertical direction, m

d_t = initial time step, yrs

N_t = maximum number of time steps

N_z = maximum number of space steps

N_L = number of leakage intervals

$A_{o,n}$ $(n=1,N_L)$ = leach rate at repository for each interval

The first part of the output list contains the input data. Then, 5 columns with data are given for each time step. These data are the z-level, the x-distance, the corresponding time, the temperature in the given point and the total velocity in this point. At the end of each time step, the following data are given:

Start time

Time for discharge of the nucleus to the surface

The z-level for the last calculated step

The leach rate for the given leakage step

The integrated leakage for the given leakage step

Typical computing times on the CYBER-172 computer are of the order 10 - 15 seconds per leakage step. Then, the initial space step was 1 meter and the initial time step 2 years.

6.2 Choise of input data

The data have been chosen with consideration of Swedish geological conditions. The geographical data have been connected to two alternatives for a repository, namely at Forsmark and at Oskarshamn. Some variations in these data have been made and the calculations can therefore be considered as a parametric study.

The largest difficulties lay in assessing the porosity values. As pointed out in Section 3, the porosity is not defined unequivocally for cracks. Furthermore, the positions of cracks with widths of the order of 1 cm or less are not very well known even for a carefully studied repository. Cracks having one or two orders of magnitude larger widths are assumed to be recognizable from the ground surface. Experimental investigations in Studsvik indicate, however, that the water velocity in a crack with about 1 cm width is about 10^{-3} m/s for unit gradient [12]. The investigated crack was then about horizontal and at a depth of about 60 m. It is reasonable to assume that vertical cracks have a better filling factor on large depths. In the calculations performed the value 10^{-3} m/s was assumed for the K_p/ϵ value at the ground surface for all large cracks. It should be noted that the largest cracks can be considered as porous media. The porosity for such cracks are assumed to have values of the same order as sandstone of high permeability. According to Lapwood [8], this is about 10^{-4} m/s and the porosity is at least as high as 0.1. Then, the velocity in very large cracks is about the same as that in cracks with a width of about 1 cm. It can also be noted that the average permeability in large cracks has been estimated to be about 10^{-5} m/s [13]. The velocity 10^{-3} m/s for unit gradient is then obtained by assuming $\epsilon = 0.01$. It is also assumed that the corresponding velocity at a depth of 1 km is 10^{-5} to 10^{-4} m/s. These values were obtained by assuming that the permeability has decreased by the factor 200 and the porosity has decreased by a factor 2 to 20. The permeability is a conservative estimation from the experimental results by Carlsson and Olsson [11]. The ϵ-values are guessed. The higher ϵ-value was obtained by assuming that 60 % of the crack is filled with a porous medium at the ground surface and that the porosity of this medium is 0.5. At 1 km depth it was then assumed that the crack is totally filled with a medium with porosity 0.35. The lowest ϵ-value is closer to those of cracks with plane parallel surfaces.

For narrow cracks, experimental permeabilities have values between 10^{-8} and 10^{-10} m/s at depths about 500 m. The porosities are, however, very uncertain. If it is assumed that the permeabilities at the ground surface are between 10^{-6} and 10^{-8} m/s and that the porosity is of the order of 10^{-3} to 10^{-5}, the K_p/ϵ values are again of the order of 10^{-3} m/s. And assuming further that a narrow crack is discharged into a large one the velocity in the former one is doubled. One conclusion is then that the velocities in narrow cracks may be greater than in broad cracks. On the other hand, narrow cracks close to a repository can be filled with clay or other sealing materials and it is therefore not possible with a higher water velocity in those cracks. Thus, the final conclusion is that it is not very meaningful to make different assumptions about the relative lengths of narrow and broad cracks. In the present calculations it was assumed that the narrow cracks start at the repository and have a length of 10 m. K_p/ϵ was assumed to have half the value taken for broad cracks. At infinity, K_p/ϵ was set to 0.1 times the value at 1 km depth. A lower boundary was set at 4 km depth.

The retardation factor, K, varies with many orders of magnitude for different nuclides. For Sr 90 the value 6 - 8 has been obtained by measurements in Studsvik [12, 13]. For illustration of the influence of K upon the migration, calculations were made in one case for K = 1, 6 and 100 with other input variables constant.

The material data connected to the heat distribution are the thermometric diffusivity κ and the volume expansion coefficient α. According to Blomquist [14], $\kappa = 0.15 \cdot 10^{-5}$ m^2/s for granite. The expansion coefficient has been chosen to $3.0 \cdot 10^{-4}$ $^oC^{-1}$ which corresponds to about 30°C. This is considered as an average value over the volume where convection occurs. The heat sources were chosen in order to satisfy the results of the calculations by Blomquist [14, 15] of the temperature distributions in hard rock due to a representa-

tive Swedish repository of radioactive wastes. He found that the maximum temperature increase above the environment temperature was in the centre of the repository at any time about 75°C. In this work, the temperature 70°C was chosen for a heat source starting at the time zero and 10°C for a source starting at the time 100 years. A decay constant of $2 \cdot 10^{-3}$ yrs^{-1} was chosen for both sources because Blomquist also found that the maximum temperature increase was about 30°C after 500 years.

The leakage time from the repository was chosen to 500 years. This is much smaller than the true leakage time but the value was chosen because the leakage is highest in the beginning. This time was divided in four parts such that migration calculations started at 0, 125, 250 and 375 years.

The initial vertical step length was chosen to 1 m and the initial step length in time was 2 years. The first time step used was calculated by the program from the velocity and the maximum vertical step length.

6.3 Geographical data and results

The geographical data are given in Figs 5 - 11 and in Table 1. Figs 5 - 7 correspond most closely to the investigated repository area at Forsmark. The real topography cannot be given exactly in two dimensions and different variants were therefore considered. The regional slope down to the Baltic is interrupted by rather horizontal levels and even by hills. But in such regions there is always a downward slope in the perpendicular direction or otherwise a lake is present. The only lake in the area cross section considered is, however, situated about 400 m from the repository in the opposite direction from the Baltic. Therefore, the most representative topography was assumed to be that of Fig 5. But, for investigation of several interruptions in the regional slope, including a hill, the topographies according to Figs 6 and 7 were considered. A simplified topography according to Fig 8

was considered in order to eliminate the influence of the first steep slope present in the earlier cases. A quite hypothetic variant with a lake in the same direction as the sea is seen in Fig 9. Fig 10 shows a repository situated quite close to the sea and with a very high regional gradient. Fig 11 shows finally a topography corresponding to an investigated site close to Oskarshamn. The real level of the lake is 1 m over the sea but the value 15 m was used in three cases for conservative reasons.

The deposition depth was normally chosen to 0.5 km but in addition the values 1.0 and 1.5 km were considered for three different topographies. It should be pointed out that no experimental values of permeabilities or porosities were available for larger depths than a few hundred meters. Therefore, the uncertainties in the results decrease for very large deposition depths.

In Table 2, the minimum times of transport to different points are given. The x-coordinates of the points were chosen as 0.25, 0.50, 1.0, 2.0 and 4.0 km. The flow was always directed towards the sea. The corresponding depths and transport times were obtained from the output from MINUTE. Theoretically, the nuclides may obtain the surface at much larger distances than 4 km but this was not considered to be of practical importance because large crossing fissures and other neglected details of the topography will effect the real migration path. In three cases, the depth is zero at some of the given points. This means that the nuclides have arrived at the surface before this point but at a time given in the corresponding time column.

Case 1 was considered for three different retardation factors, K. It is seen that the deviation from linearity in K is so small in this case that it can be neglected. Larger deviations can sometimes be found, but because of the highly approximate convection calculation it is recommended to always assume linearity.

A more detailed description of the results from case 1 is given in Figs 12 and 13. The vertical position as a function of time is given in Fig 12. The large variations in the beginning are due to the thermal convection and to the large variations in the surface slope. The depth is rather constant at larger time values because the surface is then rather smooth. Fig 13 shows the horizontal distance as a function of time and it is seen that the curve has a deviation from linearity only in the beginning.

Case 2 differs from case 1 only by a smaller value of K_p/ϵ. It should be noted that the transport times are larger for case 2 by a factor which is larger than the relation between the K_p/ϵ values. This is due to the convection effect which can be seen by comparing Figs 12 and 13 with Figs 14 and 15. The latter figures show the vertical and horizontal positions as functions of time for case 2. It is seen that the average depth is larger in case 2 than in case 1. The reason is that the temperature has decayed to a very low value within a short migration distance. One can conclude that for negligible convection the migration times would increase, especially in case 1.

Cases 3 and 4 are concerned with the same topography as cases 1 and 2 but the deposition depths are 1.0 and 1.5 km, respectively. It is seen that each step causes approximately a doubling in transport times with this topography. It will be seen later that these relations may be larger for other topographies.

In cases 5 and 6 some variations in the earlier topography are considered. It can be concluded that the occurance of a large plateau or a hill between the repository and the sea causes the water to arrive earlier to the surface. But it must be pointed out that the results are pessimistic because of the 2-dimensional model. In a 3-dimensional model there would be a slope in the perpendicular direction and this

slope will often cause a downward directed gradient besides the horizontal gradient. In any case, the last mentioned component will cause a prolonged flow path and the water will be mixed up with water from other sources.

Case 7 has the same regional slope as case 1 but the repository is situated on a place where no large local gradients occur. Because of this, the water velocity is much lower close to the repository. This conclusion is important if it is not possible to find a repository far from large fissures. Then it should be situated in an area with so low local gradients as possible. This result is still more accentuated in cases 8 and 9 which differ from case 7 with regard to the deposition depth only. In this topography, an increase in the depth by 500 meters will approximately triple the transport times.

Case 10 considers a lake between the repository and the sea. The water will then flow up into the lake but because of a comparatively large horizontal plateau. The transport times will be considerably longer than in the corresponding earlier cases. Still, the distance from the repository to the lake slope is only 750 m.

In case 11, the regional slope is 7.5 times as high as in earlier cases. It is then seen that the mean flow velocity is not proportional to this relation but is lower because of the plateau close to the repository. A similar situation is utilized in a more optimal way in cases 12 - 15. Case 12 is perhaps a little extreme because of the competition between the lake and the sea in calculating the horizontal gradient. But in cases 13 to 15 the effect of the lake is very small. Still, the average horizontal velocity for case 13 is $4.6 \cdot 10^{-8}$ m/s which corresponds to an average horizontal gradient of less than 10^{-3}. The regional gradient is $4.25 \cdot 10^{-3}$. An increase of the deposition depth from 0.5 to 1.0 km increases the transport time

by a factor of 3 in average but the gain is much larger for short transport lengths.

Additional calculations were made for case 1 with a pumped well situated at different distances from the repository. The horizontal dimensions of the well was 5 x 5 m and the depth was 5 m below the ground water surface. The well had no effect upon the migration path. The pumping will of course maximize the effect.

Another type of problems occur when the water flow with nuclides is discharged into a fissure. In this connection the following problems were considered:

a) How strong is the upward gradient in a fissure as a function of the depth if the only piezometric head is due to the decrease in the groundwater surface in the fissure compared to a constant level on both sides of the fissure? Is this gradient of importance for estimation of the point where nuclides discharged into the fissure will reach the surface?

b) Assume that the fissure is at the lower end of a slope to a valley. The upward gradient is largest at this point. How strong is then the vertical gradient for realistic topographic conditions? How long way will the nuclides move along the fissure before they reach the surface?

In both cases, it was assumed that a constant horizontal gradient exists along the fissure. It is also assumed that water is discharged into the fissure at every point so that the water from the repository will be continuously diluted. Another question is then how much the water from the repository is diluted when it reaches the surface or a well.

Consider firstly a fissure on a horizontal ground level. The geometry and boundary conditions are then according to Fig 2. For simplicity the lower boundary is extended to infinity. It is easily seen that the vertical gradient at the centre of the fissure is given by

$$\frac{1}{g}\frac{\partial\psi}{\partial z} = \frac{4\ x_s}{\pi\ z_s}\left[\left(\frac{x_s}{z_s}\right)^2 + \left(\frac{2\ z}{z_s}\right)^2\right]^{-1} \qquad (6,1)$$

Fig 16 shows the expression

$$f = \frac{z_s}{g x_s}\frac{\partial\psi}{\partial z}$$

as a function of z/z_s.

A high estimation for z_s is 1 m and the calculations have shown that the migration depth for nuclides is approximately equal to the burial depth until they arrive at a valley, lake or sea. Thus, if a burial depth of 500 m is assumed, z/z_s is at least equal to 500. Then,,

$$\frac{\partial\psi}{\partial z} \approx 1.3 \cdot 10^{-6}\ \frac{x_s}{z_s} \qquad (6,2)$$

The ratio x_s/z_s is surely less than one. The horizontal gradient is at the Forsmark site about $2 \cdot 10^{-3}$. It is then obvious that the vertical gradient is negligible for fissures of reasonable dimensions. For each meter in the upward direction, the nuclides have moved at least 1 km in the horizontal direction if no other gradients were present.

Next, consider one side of a valley with dimensions according to Fig 3. It is firstly assumed that the perpendicular extension is infinite. The vertical gradient has its largest positive value at $x = x_s$ and can be obtained from Eq (5,16) as

$$\frac{1}{g}\frac{\partial\psi}{\partial z} = \frac{z_s}{2\pi x_s}\ \ln\left[1 + \left(\frac{x_s}{z}\right)^2\right] \qquad (6,3)$$

Assume further that a large fissure is situated in the perpendicular direction at the x-value considered and that the water flow changes from the x-direction to the perpendicular y-direction because of the high permeability of the fissure. The discharge point is given by the coordinates x_s, y_o and $-z_o$. At each later moment, the relationship between the vertical and the horizontal position is given by

$$\int_{-z_o}^{-z} \frac{dz}{v_z} = \int_{y_o}^{y} \frac{dy}{v_y} \qquad (6,4)$$

where v_z and v_y are the vertical and the horizontal velocities, respectively. If the horizontal velocity is constant, the horizontal transport path can be written as

$$\Delta y = y - y_o = ig \int_{-z_o}^{-z} \frac{dz}{\left(\frac{\partial \psi}{\partial z}\right)} \qquad (6,5)$$

where i is the horizontal gradient.

Within small vertical intervals, $\partial\psi/\partial z$ can be considered as constant. Eq (6,5) can then be integrated numerically using Eq (6,3) for $\partial\psi/\partial z$. This gives a low estimation of the horizontal path length Δy for a given vertical transport path because the slope boundary always has a finite extension in the y-direction. When the boundary between the slope and the valley is replaced by a smooth surface, the vertical gradient decreases significantly.

At the Forsmark site, a large fissure is situated in about the position considered. The length and height of the slope is approximately

$$x_s \approx 60 \text{ m}$$
$$z_s \approx 10 \text{ m}$$

The gradient and the horizontal movement at different depths is then given in the following table

z (meters)	$\frac{1}{g}\frac{\partial \psi}{\partial z} \times 10^{-3}$	Δy (meters)
100	8.2	40
200	2.3	120
300	1.0	250
400	0.59	400
500	0.38	1 800
750	0.17	3 600
1 000	0.10	

It is seen from the table that the total transport length before the nuclides have reached the surface is only about 800 meters if the initial depth is 500 meters. For 1 000 m initial depth, the transport length is, however, more than 6 km. This conclusion is important because the extent of the repository in the direction of the fissure is about 1 km. Thus, the water coming from the repository is only diluted by the amount of rainwater falling over an area equal to the repository area if the transport length is less than or equal to the length of the repository. This corresponds to a deposition depth of 500 m. If, however, this depth is 1 000 m, the water flow from all land above the fissure gives a large additional dilution. This includes water from streams and from large crossing fissures and is at least one order of magnitude larger than the diluting water from the repository area. Furthermore, the transport time below the ground surface may be very long if the surface is smooth in the direction of the fissure.

6.5 Estimation of the accuracy

As mentioned earlier, the main uncertainty in the results is due to the uncertainty in the porosity or corresponding calculational quantity which effects the K_p/ϵ value. In order to point out this uncertainty, calculations were made with two values of K_p/ϵ which differ by one order of magnitude at 1 km depth. The difference is, however, lower at most of the migration paths considered. Most calculations are made with $K_p/\epsilon = 10^{-4}$ m/s at 0.5 km depth and this value is believed to be an upper limit. The transport times differ also by about one order of magnitude for the two assumptions made.

Another source of uncertainty is the crude estimation of the convection flow. Additional calculations have shown that a doubling of the flow velocity due to convection decreased the migration time by about 20 %. Such a doubling is, however, quite unreasonable for the flow from the centre of the repository

where the temperature is highest. The cirkulation paths will be shortest at the edges of the repository. There, the temperature is about 50 % of that existing in the centre. Then, changing the k-factor in Eq (4,11) from 3 to 1 and dividing the temperature difference by 2 results in an unchanged convection velocity.

The analytical models for calculating the hydraulic gradient have of course inherent approximations. The most important of these are:

a) The geometry is 2-dimensional and the ground surface is approximated by straight lines. This is at least partially compensated by considering a large number of cases.

b) The piezometric head is calculated as a linear combination of solutions for constant permeability and for an exponentially decaying permeability. The true function describing the permeability variation with the depth is not known. Furthermore, the permeability is probably anisotropic. It is not unreasonable to assume that the corresponding uncertainty in migration time is of the order of 50 %.

c) A lower boundary was set at a depth of 4 km. It is not justified to have a boundary at a smaller depth than this value. A calculation was also made for a boundary at 6 km depth. The resulting migration times were only about 1 % larger. The conclusion is that the position of the boundary is unimportant within reasonable limits.

d) The groundwater level has a large number of smaller variations in height which have not been considered. It has, however, been shown that a well with reasonable dimensions will not cause any disturbance in the flow at the depth we are concerned with here. The same conclusion must then also be valid for comparable groundwater variations. Larger variations in the surface level can be handled in the same way as lakes.

7. CONCLUSIONS

The conclusions are very much dependent upon the assumption about the ratio between permeability and porosity and upon

the retardation factors for different nuclides. If the lower value used for K_p/ϵ is valid and if the retardation factors published by Burkholder [2] hold, the underground migration times are more than 30 times the half lifes for nearly all radioactive waste nuclides in all cases. Much lower retardation factors have, however, been obtained for actinides in Swedish measurements. Then, many nuclides can never be totally stopped by absorption in the rock. It should be noticed, however, that for the most pessimistic assumption about K_p/ϵ the water transport time for a distance of 1 km is for the Forsmark site about 100 years for a deposition deoth of 0.5 km and about 200 years for a deposition depth of 1 km. The corresponding values for the Oskarshamn site are 120 years and 400 years, respectively. It was not expected that the latter site would be more favourable, because the regional gradient is higher. This is, however, more than compensated by the lower local gradient close to the repository. Still longer transport times occur for sites with very small local gradients. The regional gradient is important only over large distances and then other factors are more significant, namely, the occurence of large fissures, lakes and streams.

It was also concluded that a large fissure is not disastrous if the deposition depth is large. Then, the flow path within the fissure will be long and the water from the repository will either be highly diluted or the transport time within the fissure may be large or both can happen. A well in a valley or in a fissure has no influence upon the migration path.

It can also be concluded that the vertical gradient always is largest at a change in the surface slope and decreases rapidly with the distance from such a point. It is upward directed when the horizontal gradient decreases and vice versa. For the topographies concerned, vertical gradients may be neglected at distances larger than about 1 km from significant changes in the local horizontal gradient.

A related result was that a lake at a distance of 0.5 km or more in the opposite direction to the sea could not change the direction of the water flow.

There are uncertainties in the calculational models but these are compensated by the large number of cases considered and they are in any case small compared to the uncertainties in the geological input data. Measurements of pore velocities in a large number of cracks of varying dimensions and at different depths would be most valuable.

REFERENCES

1. HÄGGBLOM H
Diffusion of soluble materials in a fluid filling a porous medium.
AB Atomenergi internal report AE-RF-77-3231 (1977).

2. BURKHOLDER H C, DE FIGH-PRICE C
Diffusion of Radionuclide Chains through an Adsorbing Medium.
BNWL-SA-5787 (1977).

3. COLLINS R E
Flow of Fluids through Porous Materials.
Reinhold Publishing Corporation, New York, (1961).

4. BEAR J, ZASLAVSKY D, IRMAY S
Physical Principles of Water Percolation and Seepage.
Unesco 1968.

5. Acres Consulting Services Ltd.
Radioactive Waste Repository Study.
Geochemistry, AECL 1976.

6. de MARSILY G, LEDOUX E, BARBREAU A, MARGAT J
Nuclear Waste Disposal. Can the Geologist Guarantee Long-Term Isolation?
Unpublished documentation.

7. LOUIS C
Étude des écoulements d'eau dans les roches fissurées et de leurs influences sur la stabilité des massifs rocheux.
Bull. de la Direction des etudes et recherches, Serie A, No 3 (1968).

8. LAPWOOD E R
Convection of a Fluid in a Porous Medium.
Proc. Cambridge Phil. Soc., 44, 508 (1948).

9. SCHIMMEL W P, JR et al
Thermal Convection from a Localized Heat Source in Deep Ocean Sediments.
SAND76-1212, Sandia Laboratories (1976).

10. DAVIES S N, TURK L J
Optimum Depth of Wells in Crystallic Rocks.
Ground Water.
Vol 2 No 2 (1964).

11. CARLSSON A, OLSSON T
Determination of the permeability in Rock by Water Loss Measurements (In Swedish).
Vannet i Norden, 9, No 3 (1976).

12. KLOCKARS
The State Geological Research Institute, Sweden.
Private communication.

13. BROTZEN O
The State Geological Research Institute, Sweden.
Private communication.

14. BLOMQUIST R
Temperature perturbations in hard rock caused by an underground repository of radioactive waste (In Swedish).
AB Atomenergi internal report TPM-RV-375 (1974).

15. BLOMQUIST R
Preliminary calculations of the temperature distribution at a radioactive waste repository in hard rock (In Swedish).
AB Atomenergi internal report TPM-RV-454 (1977).

16. MORSE P M, FESHBACK H
Methods of Theoretical Physics.
Vol I - II
Mc Graw - Hill, New York (1953).

Table 1 Input data defining the different cases

Case	Ref Fig	Depos depth km	10^4Kp/E at depos depth	Geographical data					
				Distance in km to				Lake dim/km	
				Slopes	Plateaus	Lake	Sea	X_L	Y_L
1	5	0.5	1.0	0.6,1.0	0.66	-0.4	15.0	1.0	5.0
2	5	0.5	0.33	0.6,1.0	0.66	-0.4	15.0	1.0	5.0
3	5	1.0	0.33	0.6,1.0	0.66	-0.4	15.0	1.0	5.0
4	5	1.5	0.10	0.6,1.0	0.66	-0.4	15.0	1.0	5.0
5	6	0.5	1.0	0.6,1.9, 5.0	0.66,3.0	-0.4	15.0	1.0	5.0
6	7	0.5	1.0	0.6,1.0, 1.8,2.2	0.66,1.2,2.0	-0.4	15.0	1.0	5.0
7	8	0.5	1.0	0.0	0.0	-0.8	15.0	1.0	5.0
8	8	1.0	0.33	0.0	0.0	-0.8	15.0	1.0	5.0
9	8	1.5	0.10	0.0	0.0	-0.8	15.0	1.0	5.0
10	9	0.5	1.0	2.0	0.0	0.8	15.0	1.0	5.0
11	10	0.5	1.0	0.25,1.2	0.80	-1.0	2.0	0.0015	0.050
12	11	0.5	1.0	0.25,2.0	0.80	-1.0	4.0	1.0	1.0
13	11	0.5	1.0	0.25,2.0	0.80	-1.0	4.0	1.0	1.0
14	11	1.0	0.33	0.25,2.0	0.80	-1.0	4.0	1.0	1.0
15	11	1.5	0.10	0.25,2.0	0.80	-1.0	4.0	1.0	1.0

Table 2. Minimum time of transport (yrs) to different points given by the horizontal and vertical coordinates (km).

Case	Retard fact K	X = 0.25 -z km	t yrs	0.50 -z km	t yrs	1.0 -z km	t yrs	2.0 -z km	t yrs	4.0 km -z km	t yrs
1	6.0	0.49	280	0.55	386	0.57	578	0.36	1300	0.30	260(
1	1.0	0.45	30	0.57	65	0.56	95	0.36	225	0.31	57(
1	100.0	0.59	4700	0.65	6800	0.69	9000	0.61	25000	0.54	7000(
2	6.0	0.55	3000	0.60	3500	0.65	4070	0.53	7100	0.51	1400(
3	6.0	0.92	500	0.94	700	0.99	1300	0.89	3000	0.82	690(
4	6.0	1.40	1100	1.49	1900	1.52	3000	1.41	6800	1.35	1600(
5	6.0	0.48	280	0.56	400	0.60	540	0.31	1600	0	300
6	6.0	0.48	300	0.55	440	0.53	670	0	1080		
7	6.0	0.38	350	0.40	550	0.44	1000	0.48	1700	0.50	300(
8	6.0	0.85	1100	0.86	1700	0.90	3200	0.93	5000	0.95	800(
9	6.0	1.43	3100	1.46	4800	1.49	9000	1.52	13000	1.54	2300(
10	6.0	0.30	1000	0.41	1700	0.48	2100	0	3000		
11	6.0	0.50	70	0.54	115	0.57	200	0.59	320	0	94(
12	6.0	0.44	270	0.49	470	0.48	860	0.55	2300	0.68	320(
13	6.0	0.44	190	0.48	330	0.46	700	0.53	2100	0.65	290(
14	6.0	0.91	1100	0.95	1600	0.98	2500	1.03	5900	1.12	790(
15	6.0	1.50	3300	1.57	4800	1.55	7300	1.52	1300	1.65	2000(

Fig 1. Geometry and boundary conditions for a well.

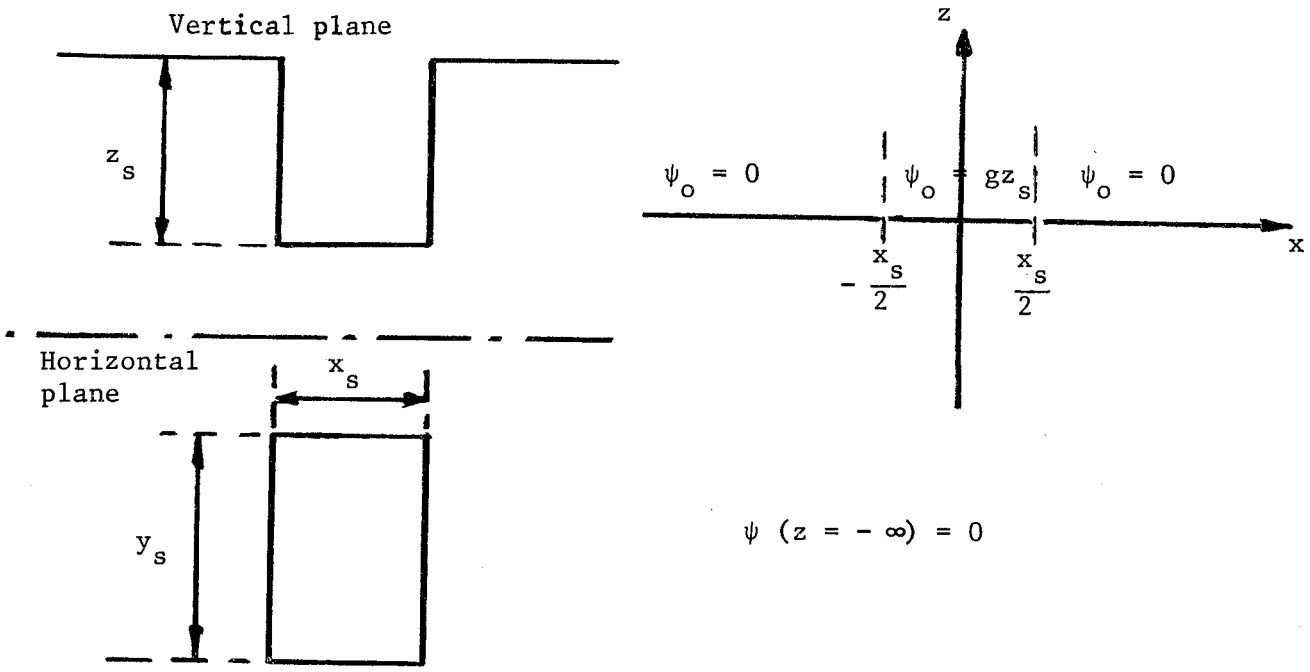

$\psi\ (z = -\infty) = 0$

Fig 2. Geometry and boundary conditions for a simplified lake or valley.

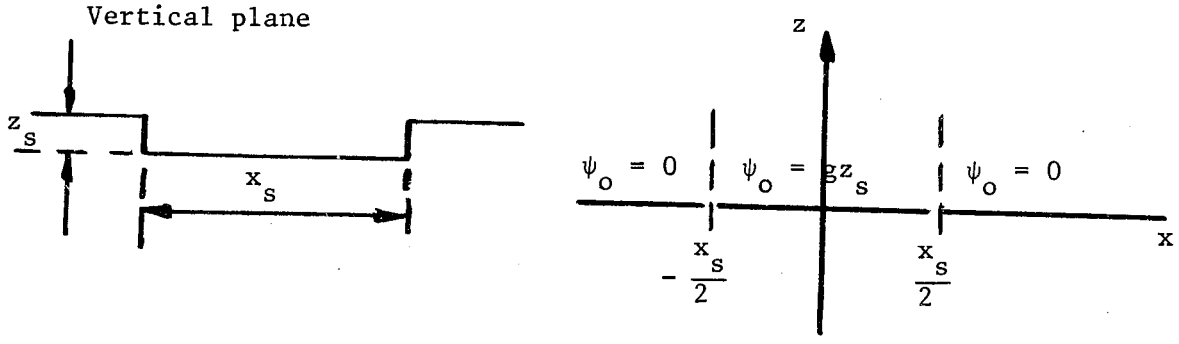

$\psi\ (z = -\infty) = 0$

Fig 3. Geometry and boundary conditions for a sea with shore slope.

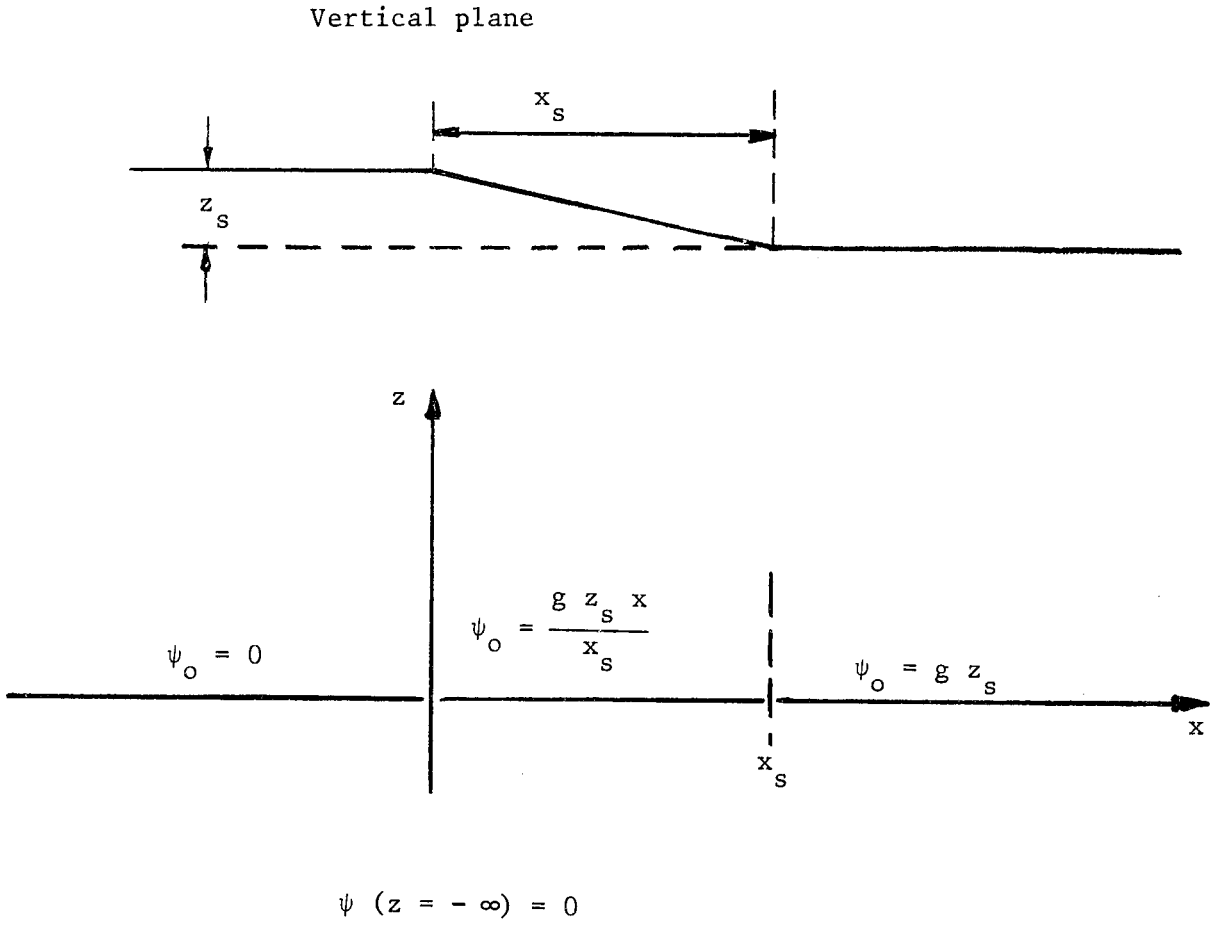

$$\psi\ (z = -\infty) = 0$$

Fig 4. Geometry and boundary conditions for general 2-dimensional topography.

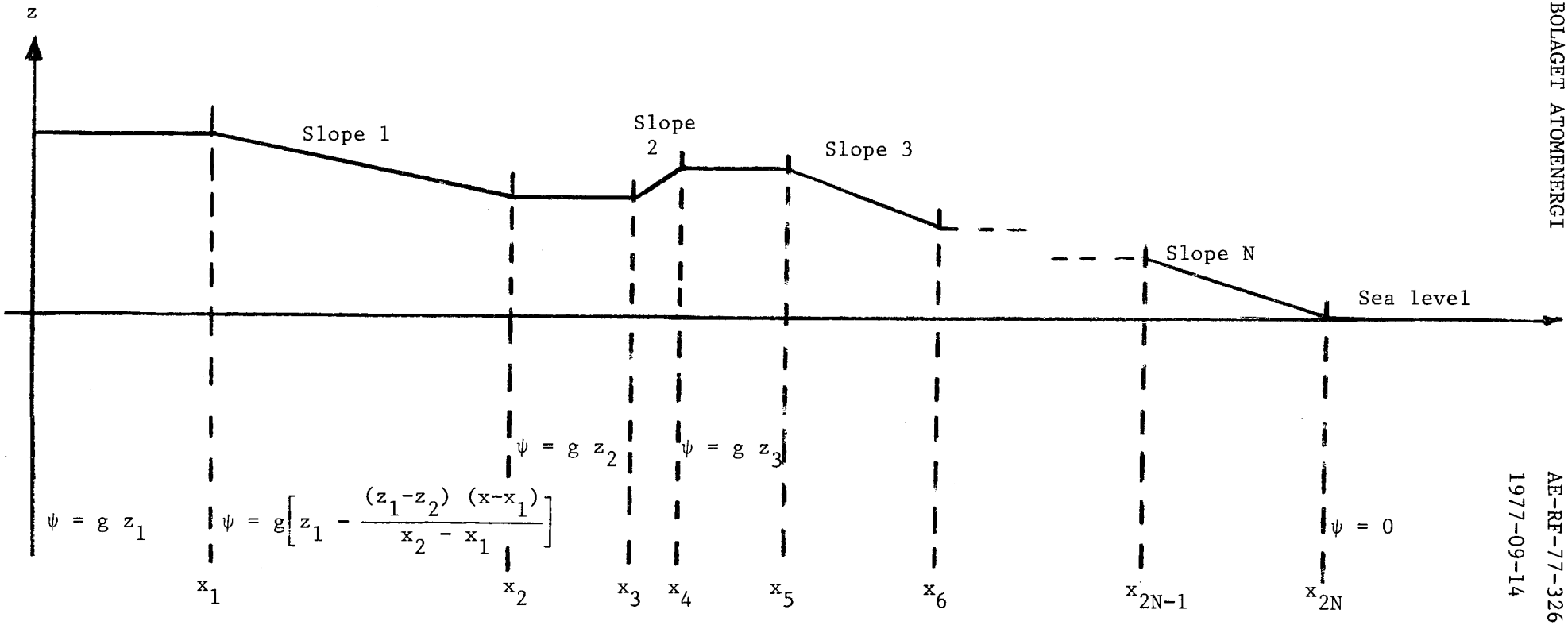

$$\left(\frac{\partial \psi}{\partial z}\right)_{z=-z_{max}} = 0$$

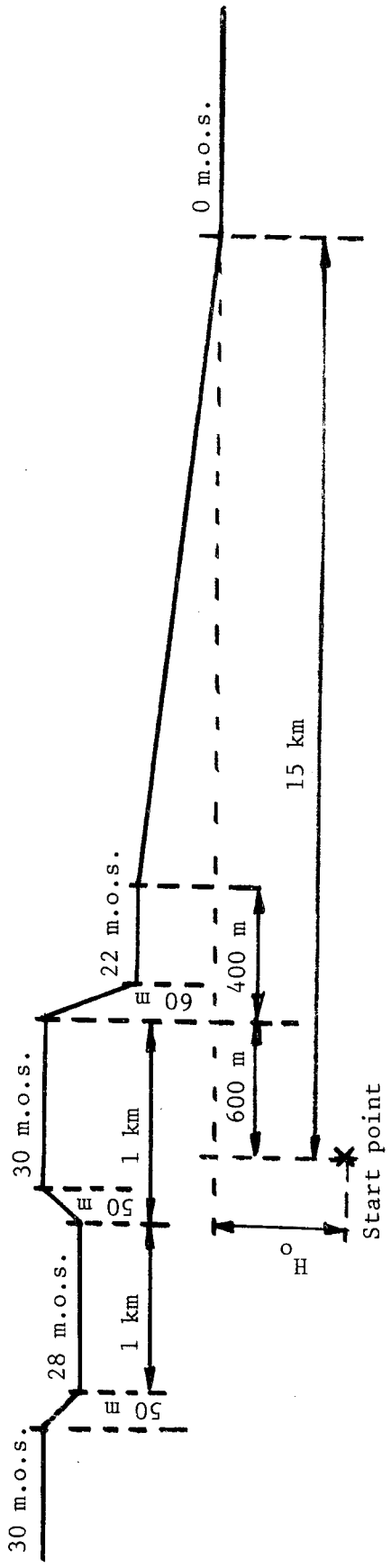

Fig 5. Topography for site A.

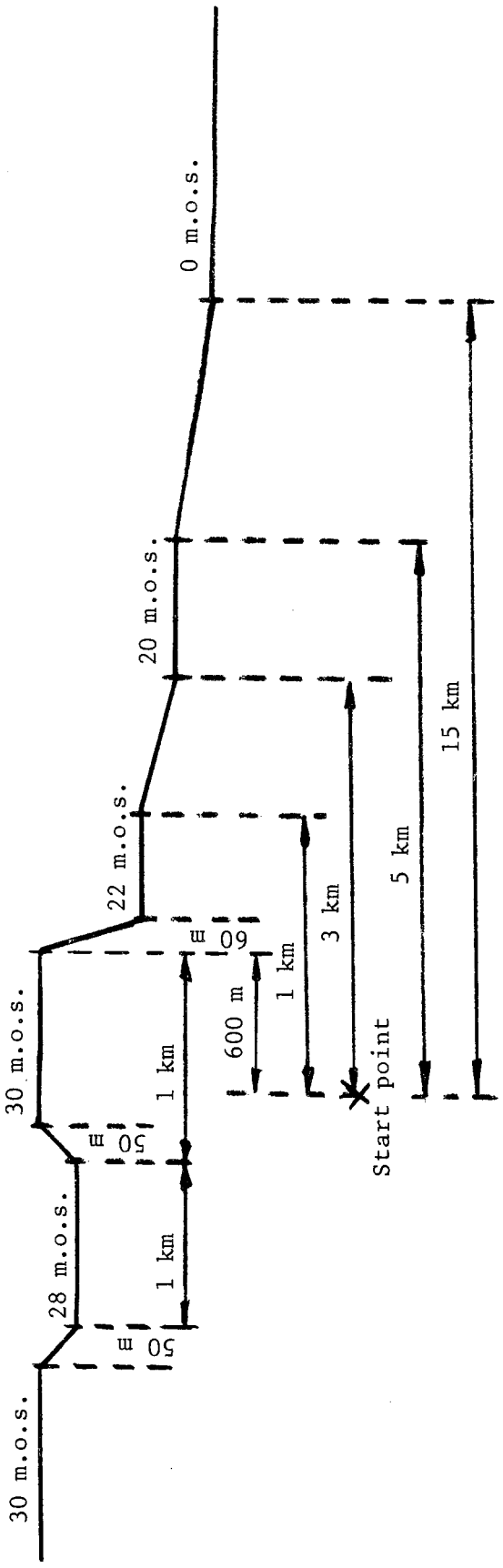

Fig 6. Topography for site B1.

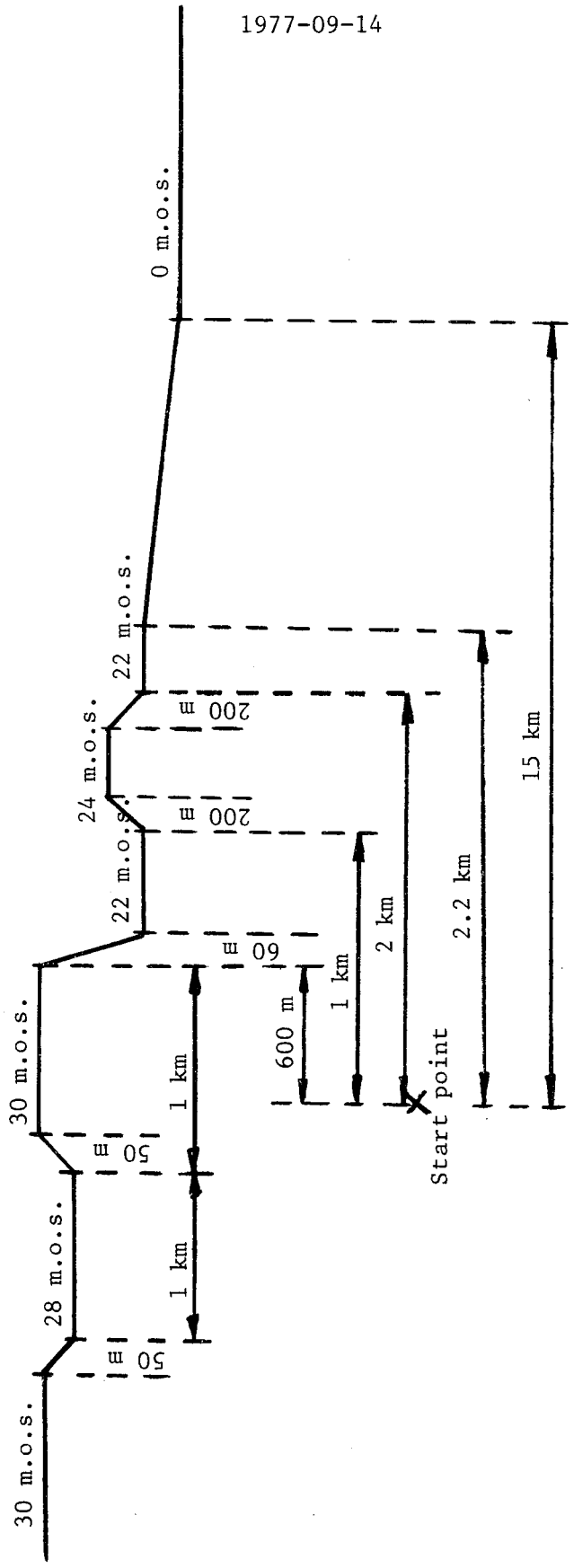

Fig 7. Topography for site B2.

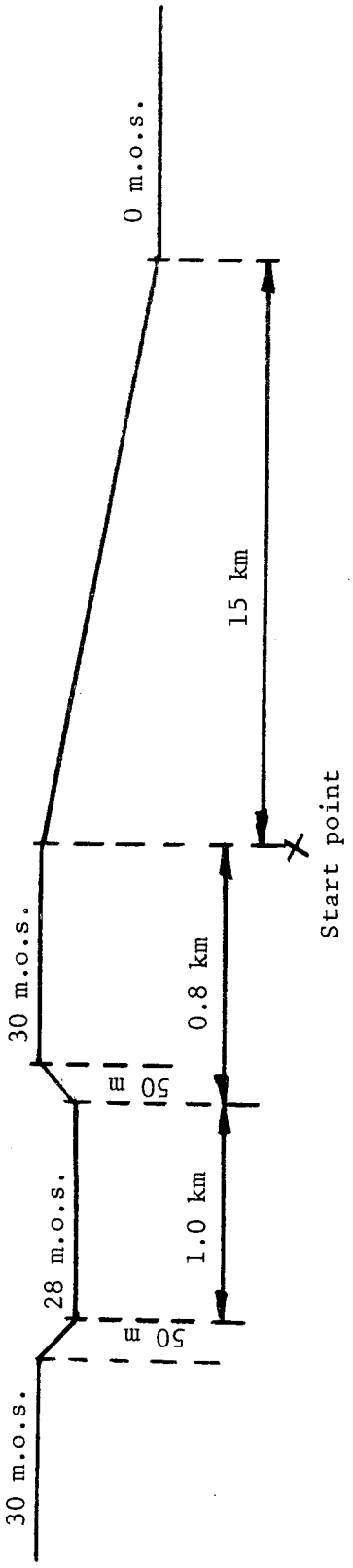

Fig 8. Topography for site C.

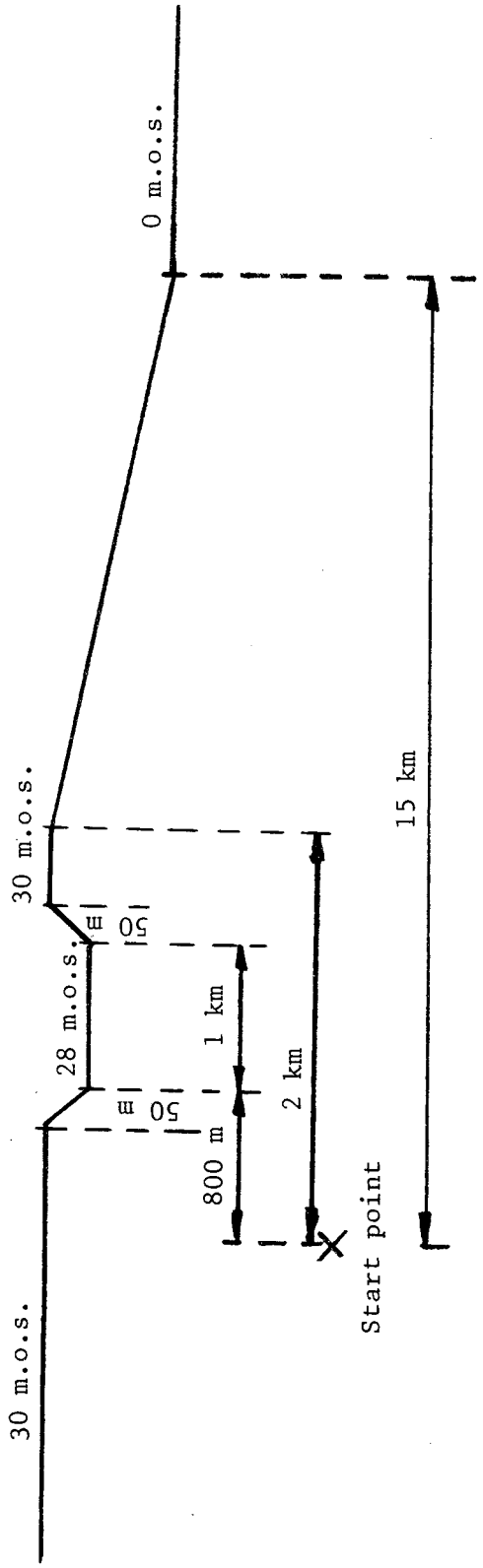

Fig 9. Topography for site D.

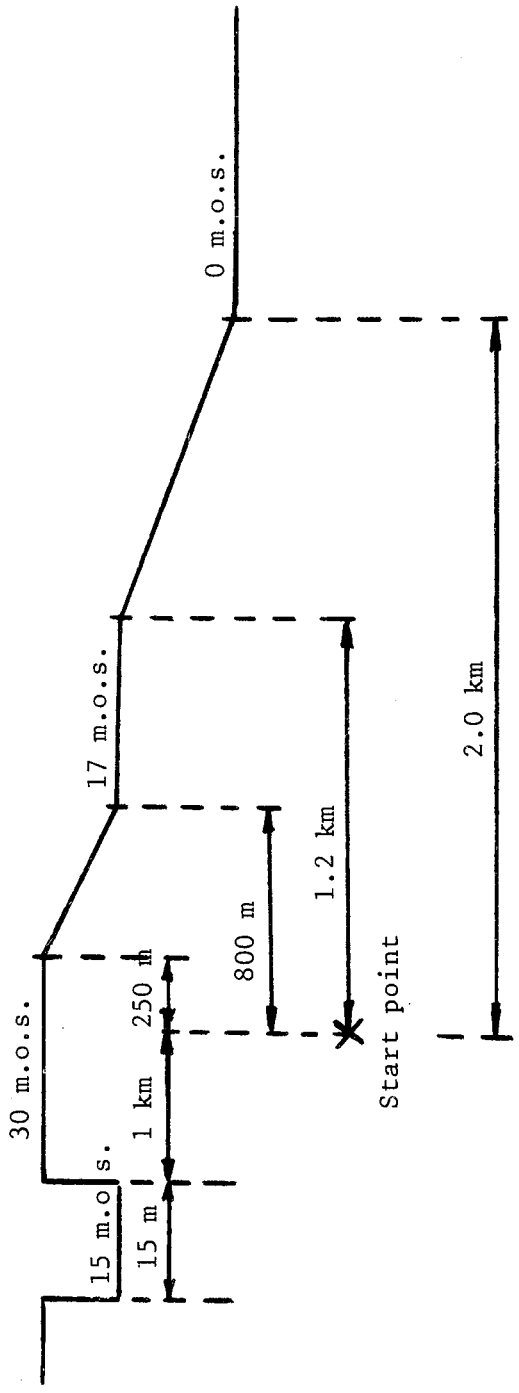

Fig 10. Topography for site E.

Fig 11. Topography for site F.

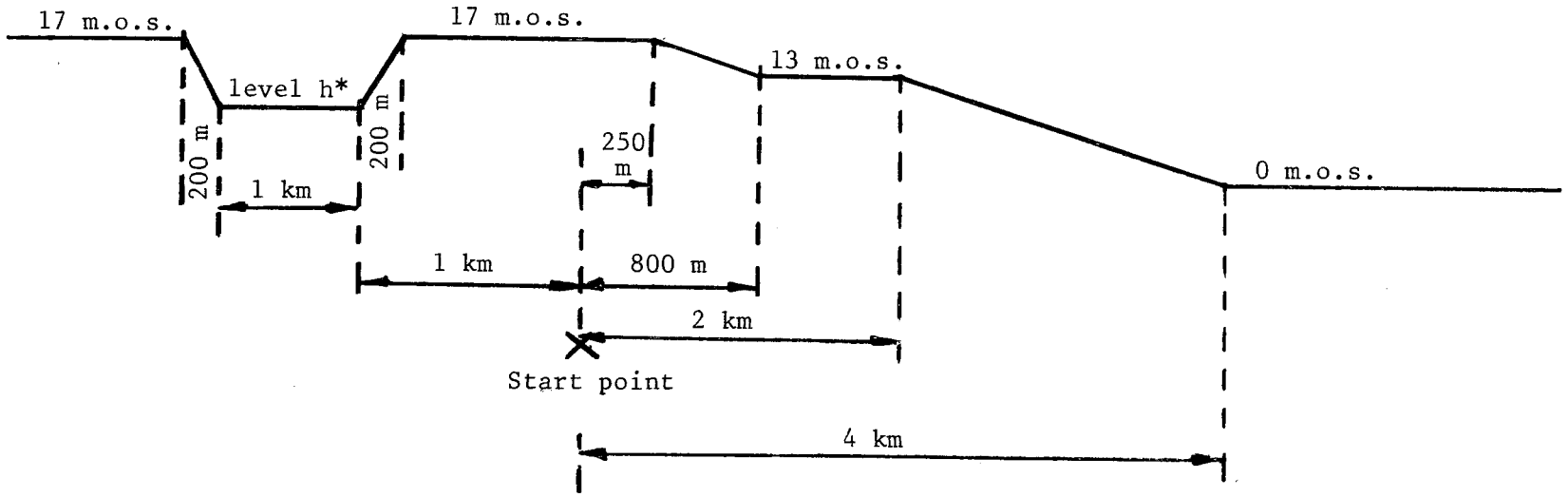

* h = 1 m.o.s. for case 12

h = 15 m.o.s. for case 13 - 15

Fig 11

Sr 90
K = 6.0
Case 1

Fig 12. Vertical position as a function of time. Topology according to Fig 5. Depos. depth 500 m.

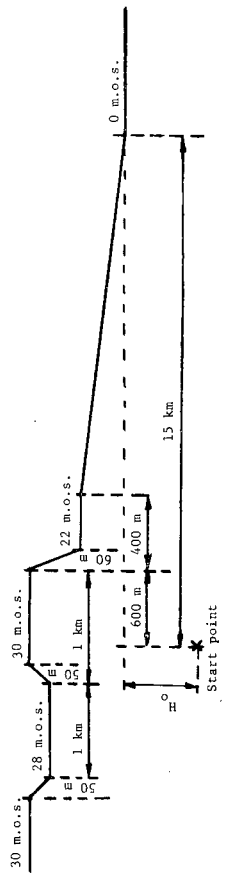

Fig 5. Topography for site A.

Sr 90
K = 6.0
Case 1

Fig 13. Horizontal distance as a function of time.
Topology according to Fig 5.
Depos. depth 500 m.

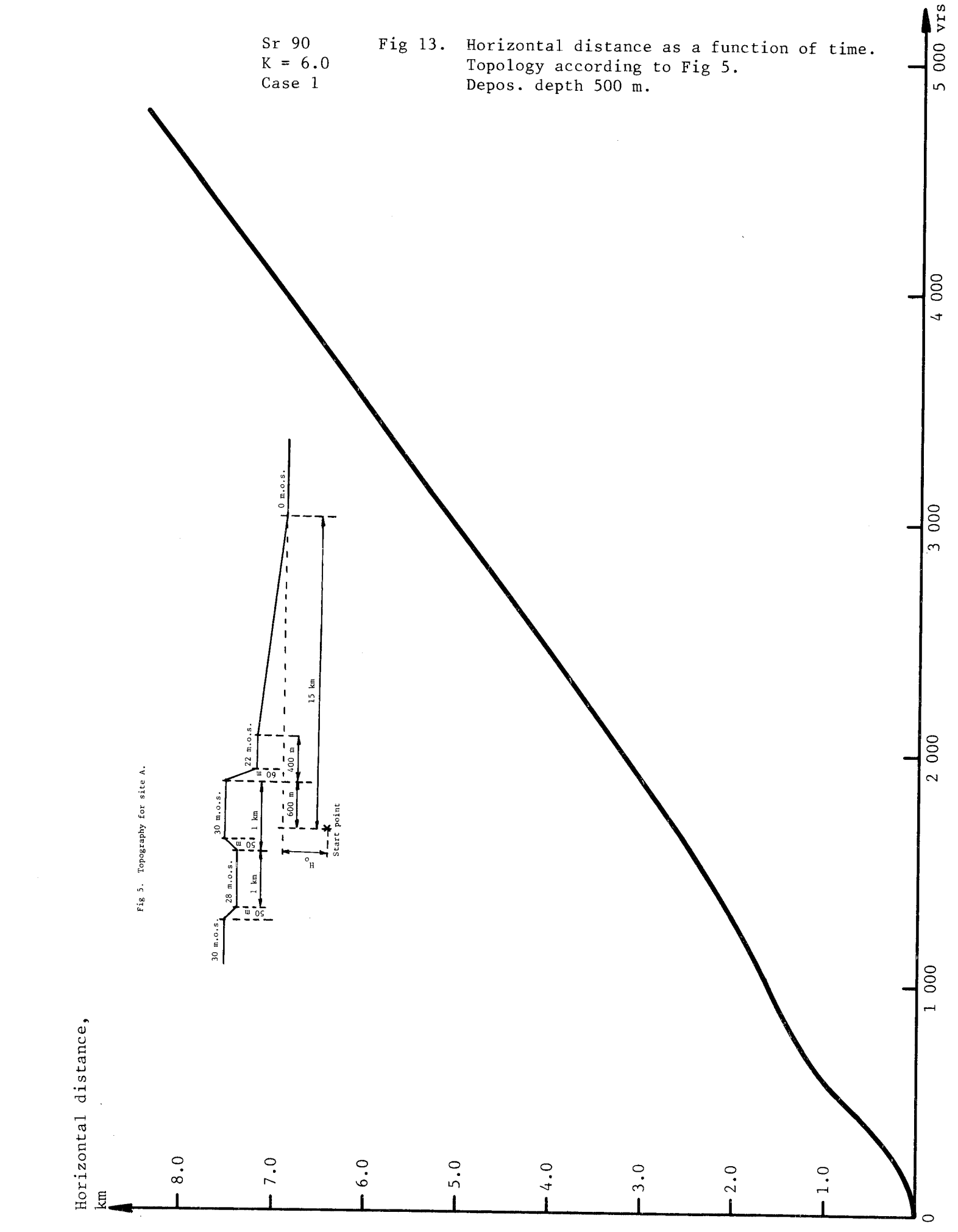

Fig 5. Topography for site A.

Sr 90
K = 6.0
Case 2

Fig 14. Vertical position as a function of time. Topology according to Fig 5. Depos. depth 500 m.

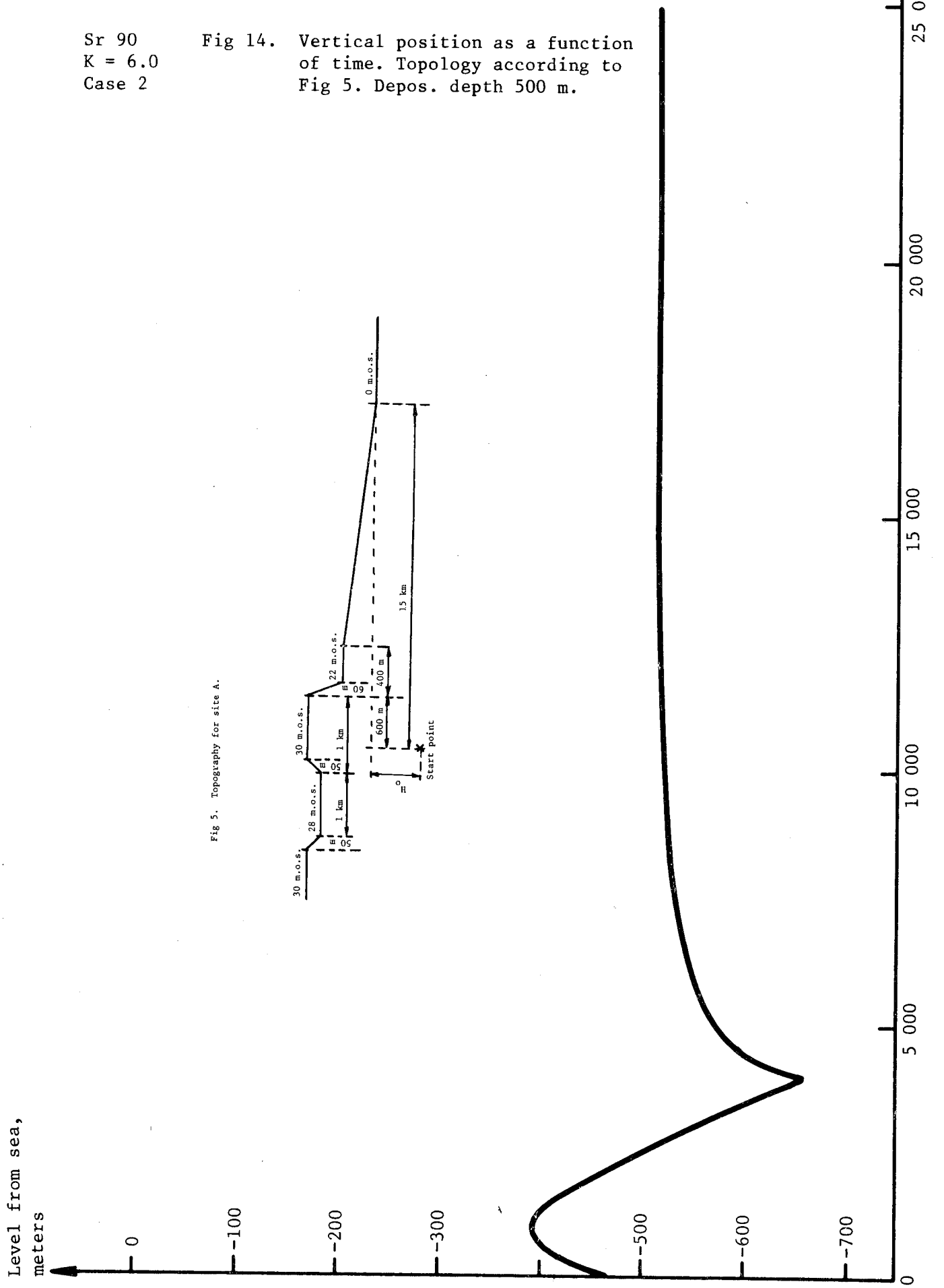

Fig 5. Topography for site A.

Sr 90
K = 6.0
Case 2

Fig 15. Horizontal distance as a function of time. Topology according to Fig 5. Depos. depth 500 m.

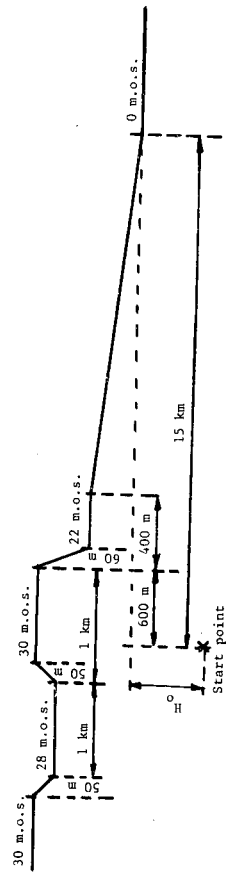

Fig 5. Topography for site A.

Fig 16. Vertical gradient in a fissure

$$f = \frac{x_s}{g\, x_s} \frac{\partial \psi}{\partial z}$$

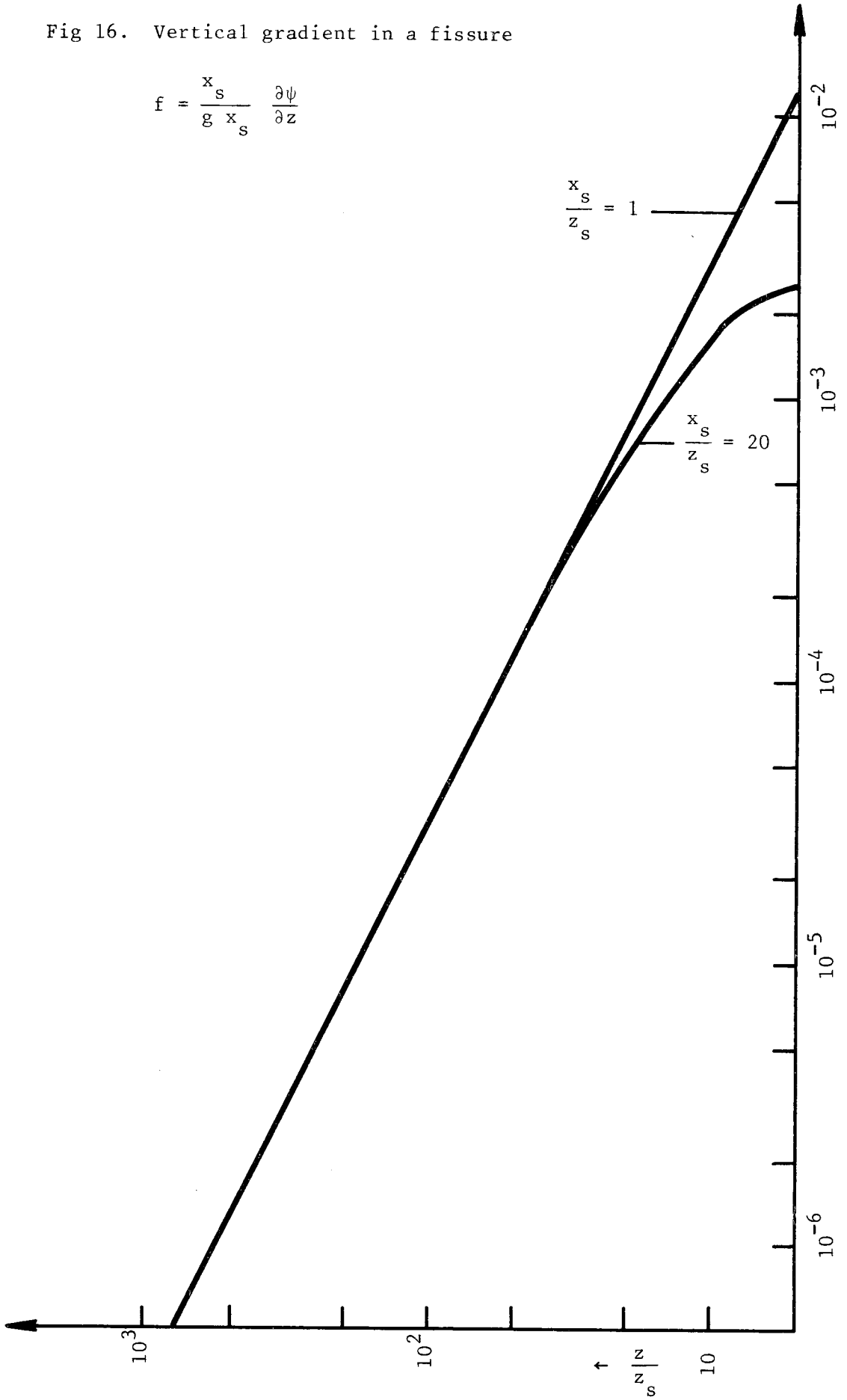

Solution of the Laplace equation for boundary conditions at x = 0 and x = - ∞

The Laplace equation in 3-dimensional Cartesian coordinates is

$$\frac{\partial^2\psi}{\partial x^2} + \frac{\partial^2\psi}{\partial y^2} + \frac{\partial^2\psi}{\partial z^2} = 0 \qquad \text{(A1,1)}$$

The boundary conditions are given in Fig 1. The Greens function method [16] is used for the solution. The boundary conditions are satisfied by a Fourier integral of the form

$$\psi\ (x,y,z) = \frac{1}{4\pi^2} \int_{-\infty}^{\infty} d\xi \int_{-\infty}^{\infty} G\ (x,y,z,\xi,\eta)\ \psi\ (\xi,\eta,o)\ d\eta \qquad \text{(A1,2)}$$

where

$$G\ (x,y,z,\xi,\eta) = \int_{-\infty}^{\infty} e^{ik_x(\xi - x)}\, dk_x$$

$$\int_{-\infty}^{\infty} e^{ik_y(\eta - y) - z\sqrt{k_x^2 + k_y^2}}\, dk_y \qquad \text{(A1,3)}$$

By writing

$$k^2 = k_x^2 + k_y^2 \qquad \text{(A1,4)}$$

and

$$r^2 = (\xi - x)^2 + (\eta - y)^2 \qquad \text{(A1,5)}$$

The Greens function can be transformed to

$$G\ (x,y,z,\xi,\eta) = 2 \int_{-\infty}^{\infty} J_o\ (kr)\ e^{-kz}\ k\ dk \qquad \text{(A1,6)}$$

The latter integral can be evaluated as

$$G\,(x,y,z,\xi,\eta) = \frac{z}{(r^2 + z^2)^{3/2}} \tag{A1,7}$$

(see [16]). If $x > \frac{x_s}{2}$, $y < \frac{y_s}{2}$, set

$$x' = x - \xi,\ y' = \eta - y \tag{A1,8}$$

The ψ-function is then, from Eqs (A1,2) and (A1,7)

$$\psi = \frac{\psi_o}{2\pi^2} \int_{x-\frac{x_s}{2}}^{x+\frac{x_s}{2}} dx' \int_{-\left(\frac{y_s}{2}+y\right)}^{\frac{y_s}{2}-y} \frac{z\,dy'}{(z^2 + r^2)^{3/2}} \tag{A1,9}$$

Using the transform

$$x' = r\cos\alpha,\ y' = r\sin\alpha \tag{A1,10}$$

Eq (A1,9) can be written

$$\psi = \frac{\psi_o z}{2\pi^2}\left[\int_0^{\arctg\left(\frac{\eta_o}{\xi_1}\right)} d\alpha \int_{\xi_o/\cos\alpha}^{\xi_1/\cos\alpha} \frac{r\,dr}{(z^2 + r^2)^{3/2}} + \right.$$
$$\left. + \int_{\arctg\left(\frac{\xi_o}{\eta_o}\right)}^{\arctg\left(\frac{\xi_o}{\eta_o}\right)} d\alpha \int_{\xi_o/\sin\alpha}^{\eta_o/\cos\alpha} \frac{r\,dr}{(z^2 + r^2)^{3/2}}\right] \tag{A1,11}$$

where

$$\xi_o = x - \frac{x_s}{2} \tag{A1,12}$$

$$\xi_1 = x + \frac{x_s}{2} \tag{A1,13}$$

$$\eta_o = \frac{y_s}{2} - y \tag{A1,14}$$

$$\eta_1 = \frac{y_s}{2} + y \tag{A1,15}$$

The integrals can be solved analytically and the final solution is given by Eqs (5,4) and (5,5). The corresponding solution for

$$x < \frac{x_s}{2}$$

is obtained by using the variable $x'' = \xi - x$ in place of x'.

The 2-dimensional Laplace equation with boundary conditions according to Fig 3 can be solved in a quite similar way. The Greens function is

$$G(x,\xi,z) = \frac{1}{\pi}\int_0^\infty e^{-k|z|}\cos[k(x-\xi)]\,dk \qquad (A1,16)$$

By using a Fourier integral over the x-axis the solution for negative z-values can be written as

$$\psi(x,z) = -\frac{1}{\pi z}\left[\frac{1}{x_s}\int_{-x}^{x_s-x}\frac{z_s(\xi+x)}{1+\left(\frac{\xi}{z}\right)^2}\,d\xi + z_s\int_{x_s-x}^{\infty}\frac{d\xi}{1+\left(\frac{\xi}{z}\right)^2}\right] \qquad (A1,17)$$

By integration, the final solution given in Eq (5,14) is obtained.

Solution of the ψ-function for boundaries at z = 0 and at a finite depth

Consider firstly the 2-dimensional Laplace equation,

$$\frac{\partial^2\psi}{\partial x^2} + \frac{\partial^2\psi}{\partial z^2} = 0 \qquad \text{(A2,1)}$$

We seek a solution which has zero z-derivative at $z = -z_{max}$ and which can be written as a Fourier integral for z = 0. This solution can be written as

$$\psi\ (x,z) = \frac{1}{2\pi}\int_{-\infty}^{\infty} \frac{\cosh\ [k(z_{max} + z)]}{\cosh\ (k\ z_{max})}\ dk$$

$$\int_{-\infty}^{\infty} e^{ik(\xi - x)}\ \psi\ (\xi,0)\ d\xi \qquad \text{(A2,2)}$$

At $k = \pm\infty$ the ψ-function behaves as e^{kz}. The integral over k may therefore be evaluated by contour integration and is equal to $2\pi i$ times the sum of the residues at all the poles of the integrand in the upper or lower half plane, depending upon the sign of $\xi - x$. The solution is then for negative z-values

$$\psi\ (x,z) = -\frac{1}{z_{max}} \sum_{n=1}^{\infty} \sin\left[\frac{\pi(n - \frac{1}{2})\ z}{z_{max}}\right]$$

$$\int_{0}^{\infty} e^{-\left[\frac{\pi(n - \frac{1}{2})\ |\xi - x|}{z_{max}}\right]}\ \psi\ (\xi,0)\ d\xi \qquad \text{(A2,3)}$$

With the boundary conditions along the x-axis given by Fig 4, the integration over ψ is simple but gives different expressions depending upon the value of x. This is because the absolute value of $\xi - x$ occurs in Eq (A2,3). For $x < x_{2N}$, sums of the following type occur

$$S = \sum_{n=1}^{\infty} \frac{2}{n} \sin \left[\frac{\pi(n - \frac{1}{2})\ z}{z_{max}} \right] \qquad (A2,4)$$

For $0 \leq z \leq z_{max}$ this expression can be evaluated as $s = \pi$.

Let us now consider the equation for the piezometric head with an exponentially decreasing permeability. The diffential equation can then be written in the form

$$\frac{\partial^2 \psi}{\partial x^2} + \frac{\partial^2 \psi}{\partial z^2} + a \frac{\partial \psi}{\partial z} = 0 \qquad (A2,5)$$

One solution of Eq (A2,6) is

$$\psi_p = e^{z(k - \frac{a}{2}) + ik_o x} \qquad (A2,6)$$

where

$$k_o = \sqrt{k^2 - \frac{a^2}{4}} \qquad (A2,7)$$

In correspondence with Eq (A2,2), a solution satisfying the proper boundary conditions is then

$$\psi = \frac{e^{-\frac{az}{2}}}{\pi} \int_{-\infty}^{\infty} \frac{\cosh\ [k(z_{max} + z)]}{\cosh\ (k\ z_{max})}\ dk$$

$$\int_{o}^{\infty} e^{ik_o(\xi - x)}\ \psi\ (\xi,0)\ d\xi \qquad (A2,8)$$

In the contour integration, the branch line is not to be crossed and the result can be written in a form similar to that for a = 0, namely

$$\psi\ (x,z) = -\frac{e^{-\frac{az}{2}}}{z_{max}} \sum_{n=1}^{\infty} \sin \left[\frac{\pi(n - \frac{1}{2})\ z}{z_{max}} \right]$$

$$\int_{o}^{\infty} e^{-\left[\frac{\pi(n - \frac{1}{2})\ \mu_n z}{z_{max}} \right]}\ \psi\ (\xi,0)\ d\xi \qquad (A2,9)$$

where

$$\mu_n = \sqrt{1 + \left[\frac{a\, z_{max}}{\pi(n - \frac{1}{2})}\right]^2} \qquad \text{(A2,10)}$$

By evaluating the integral in Eq (A2,10) for the boundary conditions given by Fig 4, the result contains slowly convergent sums of the form

$$F(z) = \sum_{n=1}^{\infty} \frac{2}{n\, \mu_n} \sin\left[\frac{\pi(n - \frac{1}{2})\, z}{z_{max}}\right] \qquad \text{(A2,11)}$$

For large n, the terms on the r.h.s. of Eq (A2,11) approach the corresponding terms of Eq (A2,4). The needed number of terms in calculating F(z) can therefore be drastically decreased by writing

$$F(z) = \pi - \sum_{n=1}^{\infty} \frac{2}{n}\left(1 - \frac{1}{\mu_n}\right) \sin\left[\frac{\pi(n - \frac{1}{2})\, z}{z_{max}}\right] \qquad \text{(A2,12)}$$

This is the form used in the MINUTE program. The final expression for the ψ-function is given by Eqs (5,22) to (5,24). Its derivates were computed numerically.

FÖRTECKNING ÖVER KBS TEKNISKA RAPPORTER

01 Källstyrkor i utbränt bränsle och högaktivt avfall från en PWR beräknade med ORIGEN
Nils Kjellbert
AB Atomenergi 77-04-05

02 PM angående värmeledningstal hos jordmaterial
Sven Knutsson
Roland Pusch
Högskolan i Luleå 77-04-15

03 Deponering av högaktivt avfall i borrhål med buffertsubstans
Arvid Jacobsson
Roland Pusch
Högskolan i Luleå 77-05-27

04 Deponering av högaktivt avfall i tunnlar med buffertsubstans
Arvid Jacobsson
Roland Pusch
Högskolan i Luleå 77-06-01

05 Orienterande temperaturberäkningar för slutförvaring i berg av radioaktivt avfall, Rapport 1
Roland Blomqvist
AB Atomenergi 77-03-17

06 Groundwater movements around a repository, Phase 1, State of the art and detailed study plan
Ulf Lindblom
Hagconsult AB 77-02-28

07 Resteffekt studier för KBS
Del 1 Litteraturgenomgång
Del 2 Beräkningar
Kim Ekberg
Nils Kjellbert
Göran Olsson
AB Atomenergi 77-04-19

08 Utlakning av franskt, engelskt och kanadensiskt glas med högaktivt avfall
Göran Blomqvist
AB Atomenergi 77-05-20

09 Diffusion of soluble materials in a fluid filling a porous medium
Hans Häggblom
AB Atomenergi 77-03-24

10 Translation and development of the BNWL-Geosphere Model
Bertil Grundfelt
Kemakta Konsult AB 77-02-05

11 Utredning rörande titans lämplighet som korrosionshärdig kapsling för kärnbränsleavfall
Sture Henriksson
AB Atomenergi 77-04-18

12 Bedömning av egenskaper och funktion hos betong i samband med slutlig förvaring av kärnbränsleavfall i berg
Sven G Bergström
Göran Fagerlund
Lars Rombén
Cement- och Betonginstitutet 77-06-22

13 Urlakning av använt kärnbränsle (bestrålad uranoxid) vid direktdeponering
Ragnar Gelin
AB Atomenergi 77-06-08

14 Influence of cementation on the deformation properties of bentonite/quartz buffer substance
Roland Pusch
Högskolan i Luleå 77-06-20

15 Orienterande temperaturberäkningar för slutförvaring i berg av radioaktivt avfall
Rapport 2
Roland Blomquist
AB Atomenergi 77-05-17

16 Översikt av utländska riskanalyser samt planer och projekt rörande slutförvaring
Åke Hultgren
AB Atomenergi augusti 1977

17 The gravity field in Fennoscandia and postglacial crustal movements
Arne Bjerhammar
Stockholm augusti 1977

18 Rörelser och instabilitet i den svenska berggrunden
Nils-Axel Mörner
Stockholms Universitet augusti 1977

19 Studier av neotektonisk aktivitet i mellersta och norra Sverige, flygbildsgenomgång och geofysisk tolkning av recenta förkastningar
Robert Lagerbäck
Herbert Henkel
Sveriges Geologiska Undersökning september 1977

20 Tektonisk analys av södra Sverige, Vättern - Norra Skåne
Kennert Röshoff
Erik Lagerlund
Lunds Universitet och Högskolan Luleå september 1977

21 Earthquakes of Sweden 1891 - 1957, 1963 - 1972
Ota Kulhánek
Rutger Wahlström
Uppsala Universitet september 1977

22 The influence of rock movement on the stress/strain situation in tunnels or bore holes with radioactive consisters embedded in a bentonite/quartz buffer mass
Roland Pusch
Högskolan i Luleå 1977-08-22

23 Water uptake in a bentonite buffer mass
A model study
Roland Pusch
Högskolan i Luleå 1977-08-22

24 Beräkning av utlakning av vissa fissionsprodukter och aktinider från en cylinder av franskt glas
Göran Blomqvist
AB Atomenergi 1977-07-27

25 Blekinge kustgnejs, Geologi och hydrogeologi
Ingemar Larsson KTH
Tom Lundgren SGI
Ulf Wiklander SGU
Stockholm, augusti 1977

26 Bedömning av risken för fördröjt brott i titan
Kjell Pettersson
AB Atomenergi 1977-08-25

27 A short review of the formation, stability and cementing properties of natural zeolites
Arvid Jacobsson
Högskolan i Luleå 1977-10-03

28 Värmeledningsförsök på buffertsubstans av bentonit/pitesilt
Sven Knutsson
Högskolan i Luleå 1977-09-20

29 Deformationer i sprickigt berg
Ove Stephansson
Högskolan i Luleå 1977-09-28

30 Retardation of escaping nuclides from a final depository
Ivars Neretnieks
Kungliga Tekniska Högskolan Stockholm 1977-09-14

31 Bedömning av korrosionsbeständigheten hos material avsedda för kapsling av kärnbränsleavfall. Lägesrapport 1977-09-27 samt kompletterande yttranden.
Korrosionsinstitutet och dess referensgrupp

32 Long term mineralogical properties of bentonite/quartz buffer substance
Preliminär rapport november 1977
Slutrapport februari 1978
Roland Pusch
Arvid Jacobsson
Högskolan i Luleå

33 Required physical and mechanical properties of buffer masses
Roland Pusch
Högskolan Luleå 1977-10-19

34 Tillverkning av bly-titan kapsel
Folke Sandelin AB
VBB
ASEA-Kabel
Institutet för metallforskning
Stockholm november 1977

35 Project for the handling and storage of vitrified high-level waste
Saint Gobain Techniques Nouvelles October, 1977

36 Sammansättning av grundvatten på större djup i granitisk berggrund
Jan Rennerfelt
Orrje & Co, Stockholm 1977-11-07

37 Hantering av buffertmaterial av bentonit och kvarts
Hans Fagerström, VBB
Björn Lundahl, Stabilator
Stockholm oktober 1977

38 Utformning av bergrumsanläggningar
Arne Finné, KBS
Alf Engelbrektson, VBB
Stockholm december 1977

39 Konstruktionsstudier, direktdeponering
ASEA-ATOM
VBB
Västerås

40 Ekologisk transport och stråldoser från grundvattenburna radioaktiva ämnen
Ronny Bergman
Ulla Bergström
Sverker Evans
AB Atomenergi

41 Säkerhet och strålskydd inom kärnkraftområdet.
Lagar, normer och bedömningsgrunder
Christina Gyllander
Siegfried F Johnson
Stig Rolandson
AB Atomenergi och ASEA-ATOM

42 Säkerhet vid hantering, lagring och transport av använt kärnbränsle och förglasat högaktivt avfall
Ann Margret Ericsson
Kemakta november 1977

43 Transport av radioaktiva ämnen med grundvatten från ett bergförvar
Bertil Grundfelt
Kemakta november 1977

44 Beständighet hos borsilikatglas
Tibor Lakatos
Glasteknisk Utveckling AB

45 Beräkning av temperaturer i ett envånings slutförvar i berg för förglasat radioaktivt avfall Rapport 3
Roland Blomquist
AB Atomenergi 1977-10-19

46 Temperaturberäkningar för använt bränsle
Taivo Tahrandi
VBB

47 Teoretiska studier av grundvattenrörelser
Preliminär rapport oktober 1977
Slutrapport februari 1978
Lars Y Nilsson
John Stokes
Roger Thunvik
Inst för kulturteknik KTH

48 The mechanical properties of Stripa granite
Graham Swan
Högskolan i Luleå 1977-09-14

49 Bergspänningsmätningar i Stripa gruva
Hans Carlsson
Högskolan i Luleå 1977-08-29

50 Lakningsförsök med högaktivt franskt glas i Studsvik
Göran Blomqvist
AB Atomenergi november 1977

51 Seismotechtonic risk modelling for nuclear waste disposal in the Swedish bedrock
F Ringdal
H Gjöystdal
E S Husebye
Royal Norwegian Council for scientific and industrial research

52 Calculations of nuclide migration in rock and porous media, penetrated by water
H Häggblom
AB Atomenergi 1977-09-14

53 Mätning av diffusionshastighet för silver i lera-sand-blandning
Bert Allard
Heino Kipatsi
Chalmers tekniska högskola 1977-10-15

54 Groundwater movements around a repository

54:01 Geological and geotechnical conditions
Håkan Stille
Anthony Burgess
Ulf E Lindblom
Hagconsult AB september 1977

54:02 Thermal analyses
Part 1 Conduction heat transfer
Part 2 Advective heat transfer
Joe L Ratigan
Hagconsult AB september 1977

54:03 Regional groundwater flow analyses
Part 1 Initial conditions
Part 2 Long term residual conditions
Anthony Burgess
Hagconsult AB oktober 1977

54:04 Rock mechanics analyses
Joe L Ratigan
Hagconsult AB september 1977

54:05 Repository domain groundwater flow analyses
Part 1 Permeability perturbations
Part 2 Inflow to repository
Part 3 Thermally induced flow
Joe L Ratigan
Anthony S Burgess
Edward L Skiba
Robin Charlwood

54:06 Final report
Ulf Lindblom et al
Hagconsult AB oktober 1977

55 Sorption av långlivade radionuklider i lera och berg
Del 1 Bestämning av fördelningskoefficienter
Del 2 Litteraturgenomgång
Bert Allard
Heino Kipatsi
Jan Rydberg
Chalmers tekniska högskola 1977-10-10

56 Radiolys av utfyllnadsmaterial
Bert Allard
Heino Kipatsi
Jan Rydberg
Chalmers tkniska högskola 1977-10-15